IEEE Access
Multidisciplinary | Rapid Review | Open Access Journal

Received 21 June 2023, accepted 19 July 2023, date of publication 27 July 2023, date of current version 7 August 2023.

Digital Object Identifier 10.1109/ACCESS.2023.3299497

RESEARCH ARTICLE

Recent Trends in EEG-Based Motor Imagery Signal Analysis and Recognition: A Comprehensive Review

NEHA SHARMA[1], MANOJ SHARMA[1], (Senior Member, IEEE), AMIT SINGHAL[2], (Member, IEEE), RITESH VYAS[3], HASMAT MALIK[4,5], (Senior Member, IEEE), ASYRAF AFTHANORHAN[6], AND MOHAMMAD ASEF HOSSAINI[7]

[1]Electronics and Communication Department, Bennett University, Greater Noida 201310, India
[2]Electronics and Communication Department, Netaji Subhas University of Technology, Delhi 110078, India
[3]Department of Information and Communication Technology, Pandit Deendayal Energy University, Gandhinagar 382007, India
[4]Department of Electrical Power Engineering, Faculty of Electrical Engineering, Universiti Teknologi Malaysia, Skudai 81310, Malaysia
[5]Department of Electrical Engineering, Graphic Era Deemed to be University, Dehradun 248002, India
[6]Faculty of Business and Management, Universiti Sultan Zainal Abidin (UniSZA), Gong Badak, Kuala Terengganu, Terengganu 21300, Malaysia
[7]Department of Physics, Badghis University, Badghis 3351, Afghanistan

Corresponding author: Mohammad Asef Hossaini (asef.hossaini_edu@basu.edu.af), Asyraf Afthanorhan (asyrafafthanorhan@unisza.edu.my), and Hasmat Malik (hasmat.malik@gmail.com)

This work was supported by Intelligent Prognostic Private Limited Delhi, India, and the Universiti Sultan Zainal Abidin-UniSZA (UniSZA) Malaysia.

ABSTRACT The electroencephalogram (EEG) motor imagery (MI) signals are the widespread paradigms in the brain-computer interface (BCI). Its significant applications in the gaming, robotics, and medical fields drew our attention to perform a detailed analysis. However, the problem is ill-posed as these signals are highly nonlinear, unpredictable, and noisy, hence making it exceedingly hard to be analyzed adequately. This paper provides a first-of-its-kind comprehensive review of conventional signal processing and deep learning techniques for BCI MI signal analysis. The review comprises extensive works carried out in the domain in the recent past, highlighting the current challenges of the problem. A new categorization of the existing approaches has been presented for better clarification. An all-inclusive description of the signal processing techniques has been corroborated by relevant works in the area. Moreover, architectures of various standard deep learning algorithms along with their merits and demerits are also explicated to assist the readers. The tabular representations of the numerical results are also readily provided. This work also presents the open research problems and future directions.

INDEX TERMS Brain-computer interface (BCI), convolutional neural network (CNN), electroencephalogram (EEG), motor imagery (MI), variational autoencoders (VAE).

I. INTRODUCTION

Recent advancements in biomedical signal processing techniques in healthcare have shifted the paradigm towards the development of algorithms to attain better precision, sustainability, and less computational time. The signals obtained from various living beings due to their physiological processes are called biomedical signals [1]. There are several types of electrical signals generated by various body parts. Some of them are electrocardiogram (ECG), electromyogram (EMG), electroretinogram (ERG), electroencephalogram (EEG), and electrooculogram (EOG).

A brief overview of the recent history of biomedical signals is provided here. ECG test is performed for examining the heart's electrical activity to determine whether it is functioning properly [2]. Several types of ECG can be performed such as resting ECG, exercise ECG, and 24-hour ECG. With the help of ECG, heart diseases (heart attack, enlargement of the heart, blockage in veins), and arrhythmia can be detected. EMG is an experiment that examines the functioning of muscles and nerve cells that controls motor neurons. It takes sensory nerves and motor nerves into account to determine

The associate editor coordinating the review of this manuscript and approving it for publication was Norbert Herencsar.

whether they are functioning properly. EMG can be surface or intramuscular EMG. Its main drawbacks are that it depends on how much body fat a person has and how cooperative he is [3]. EOG is the study of the existing resting potential between the cornea and Bruch's membrane. It is used to study eye movements. During EOG, electrodes are attached to the skin on both sides of the eyes [4], [5]

In this paper, our focus is on EEG signals which allow us to investigate the brain's electrical activity [6]. These are electrical, and non-electrical signals that we can capture and monitor as shown in Table 1. But, electrical signals are preferred over non-electrical signals because of the availability of less invasive and portable machinery. The basic principle of obtaining amplitude of brain signals is by calculating the potential difference from the two electrodes that are affixed to the skin using a differential amplifier [7]. We can detect multiple diseases with the help of EEG like epilepsy, head injury, brain tumor, encephalopathy, sleep disorders, and strokes [8]. For recording EEG signal, various electrode placement methods are there such as 10-10, 10-20 [9]. Their nomenclature is generally according to the position of the electrodes. To record an EEG signal, the most commonly used method is the international 10-20 system, as shown in Fig.1. Each electrode placement site letter represents the part of the brain from where it is reading the data, for example, letters FP, F, T, O, and C stand for the frontal-parietal, frontal, temporal, occipital, and central regions of the brain, respectively. Behind the outer ear, reference electrodes A1 and A2 are used. A distance of '10' and '20' of all the skull are used to position adjacent electrodes. That is why it is termed as 10-20 electrode placement system [10]. We can record various categories of EEG such as sleep deprived EEG, ambulatory EEG, routine EEG, and video EEG. When doing routine EEG recordings, subjects are typically encouraged to relax or take a deep breath. The duration of a routine EEG is 20-30 minutes. It is immensely helpful in distinguishing seizures and epilepsy. Sleep EEG is used for sleep disorders if there is not much information available from routine EEG. Sleep EEG is performed when subject is asleep. Whereas sleep-deprived EEG provides satisfactory results while the subject acquires less sleep than usual before undergoing for the test. When recording is done throughout the day and night, then it is called ambulatory (24-hour).

Artifacts often occur during the aforementioned EEG recording owing to things like eye movement and body part movement, which might cause the EEG data to be inaccurate. This can be easily avoided with video EEG. A video EEG is the EEG in which a subject is filmed during the EEG recording. A small EEG recorder is attached to clothes so that the EEG signal can be recorded during all the activities. With the help of this, it is easy to detect the reason for the occurrence of the artifacts. The brain generates different signals for different tasks and actions. These various types of generated waves by the brain are called EEG waves (delta (δ), theta (θ), alpha (α), beta (β), and Gamma (γ)). These waves may be seen across the brain's lobes., and their frequencies and amplitudes are also different [11], [12]. Table 2 provides the comparison of EEG waves generated by the brain in accordance with frequency.

The brain-computer interface (BCI) is a system that monitors and analyzes brain signals before converting them to commands that are sent to output devices to accomplish the specified task. BCI system helps in interacting with the outside world by apprehending the brain signal [13]. Therefore, the study of BCI provides an exciting opportunity to study the correspondence between the motor movements of a person and the electrical signals of the brain. The fundamental idea underpinning BCI is to rebuild a new system rather than restoring the old one.

At divergent consideration, BCI has itself inspired different works, such as, related to hardware development, signal processing, and classification algorithms, studying the underlying neural mechanisms, and applications. There are various types of approaches for a BCI. Asynchronous and synchronous BCI are the two categories of BCIs [14]. Synchronous BCI is also called a system-paced BCI as all the procedure is done according to the system. It leads with the advantages of easy design and easy control of user artifacts. But it also yields a disadvantage that users cannot decide when to perform and when to take a rest. Asynchronous BCI is also called self-paced BCI. It is a real-time system as the user is free to relax or act according to himself. Its drawbacks include heavy computational requirements and sensitivity for artifacts. Various other paradigms of electrical brain activities are steady-state visual evoked potential, event-related P300, N400, and slow cortical potential. One of the popular BCI archetypes is motor imagery (MI) where movements are imagined to elicit neural activity [15]. BCI has produced notable accomplishments that provide patients, who are fully paralyzed and those with severe motor difficulties, with a way of communication using computers that enables their command and control over the environments [16]. It is also used in gaming and robotics for efficient work. BCILAB, MATLAB toolboxes, Open Vibe, BioSig, and EEGLAB are available online and offline tools for processing EEG data [17].

The block diagram of the EEG based BCI systems has been shown in Fig.2, where the raw signal is preprocessed, decomposed, and features are retrieved. The classifier is used to process these retrieved features. This pipeline is used for the BCI signal processing approach. The block diagram comprises of four parts as follows:

- Signal acquisition: It is the part where the signal is captured from the brain.
- Signal processing: It consists of two sub-parts, one is preprocessing, where the artifacts present in the signal are removed, and the other one is extraction of features from the clean signal.
- Classification: After signal processing, the signal must be classified in order to identify the control signal using the previously obtained features.
- Feedback/Application: It is used to provide information on the outcome of brain activity.

TABLE 1. Different techniques to acquire brain signal.

Features	Neurosurgery	ECoG	EEG	MEG	fMRI
Technique	Invasive	Partial Invasive	Non-Invasive	Non-Invasive	Non-Invasive
Signal	Electrical	Electrical	Electrical	Magnetic	Metabolic
Portability	Yes	Yes	Yes	No	No
Spatial resolution	Very high	High	Low	Medium	High
Temporal resolution	Very high	High	High	Medium	Low
Risks	Surgery needed	Surgery needed	No Risk	High Magnetic field	High Magnetic field

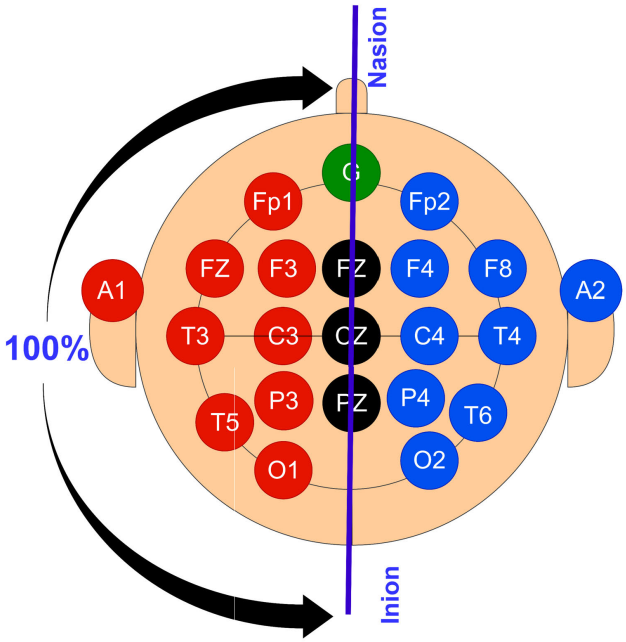

- **FP-Frontal Parietal**
- **F- Frontal**
- **P- Parietal**
- **T- Temporal**
- **C- Central**
- **O- Occipital**

- **Left axis odd number**
- **Right axis even numbers**

FIGURE 1. 10-20 electrode placement for recording EEG signal.

TABLE 2. Types of brain waves.

Type of waves	Frequency(Hz)	Amplitude(μV)	Lobe of brain	Available in
Delta (δ)	up to 4	$20-200$	Cortex/Thalamus	It appears when we are energetic after waking up.
Theta(θ)	$4-7$	10	Hippocampal	It occurs when we are disappointed.
Alpha(α)	$8-10$	$2-100$	Parietal occipital	It occurs when our mind is alert.
Beta(β)	$13-30$	$5-10$	Frontal	It occurs in the most active state like in reasoning.
Gamma(γ)	$30-100$	–	Between frontal and parietal lobe	It occurs when we combine different senses like sound and sight.

This review article builds a strong platform for research in the related domain. Our main contributions are listed below:

- A new perspective to categorize existing techniques for MI-EEG signals.
- An exploratory overview of conventional signal decomposition approaches and deep learning methods for MI-EEG signal analysis is discussed.
- The review comprises of extensive discussion on the existing works and the active challenges in MI-EEG signal analysis.
- Additionally, open research problems and future directions for MI-EEG signals are also presented.

The various techniques used for MI-EEG signal analysis are listed in Fig. 3. MI signals can be processed with conventional signal processing techniques as well as deep learning based techniques. In conventional techniques, raw EEG data is provided for processing, where it is either decomposed or transformed to another domain. From the resultant output, various attributes are extracted and given to classifiers for predicting the class of the input signal. However, in deep learning based techniques, raw EEG signal is fed to the deep neural network (DNN) which extracts features and classifies the signal automatically by optimizing the loss function.

This article is presented in the following structure: Section II includes the brief overview of the prepossessing of the signal where various artifacts, reason of occurrence, and method of removal are discussed along with signal processing techniques. Additionally, feature selection and feature transformation are discussed where selected features

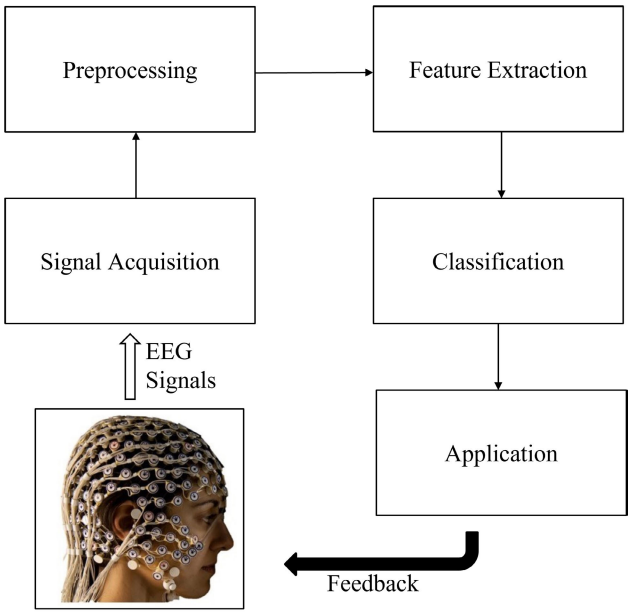

FIGURE 2. Block diagram for EEG signal processing.

are passed through various classifiers. Deep learning-based techniques are also discussed in this section. Section III contains detailed study of various databases of EEG signals. Furthermore, Section IV includes performance measures that are used for the evaluation of the signal. Section V comprises of a comparison of the state-of-the-art (SotA) conventional signal processing and deep learning techniques. Thereafter, Section VI presents the challenges associated with MI-EEG data, and recent trends and applications are also discussed. Finally, Section VII provides a summary and critique of the findings.

II. ALGORITHMS FOR MI-EEG ANALYSIS

The MI-EEG Analysis techniques can be categorised as: conventional approaches and deep learning-based approaches, as shown in Fig. 3. These approaches are discussed in detail as follows.

A. CONVENTIONAL APPROACH FOR MI-EEG RECOGNITION TECHNIQUES

In the conventional approach, the signal is preprocessed before applying signal decomposition techniques. Feature extraction, feature dimensionality reduction, and feature selection processes are performed on the decomposed signal before passing it to the classifier. All these processes are aligned to fulfill the criteria of the optimal classification result. The conventional signal processing techniques are usually employed to analyse, characterize, and investigate the EEG signals.

The categorization of distinct signal processing techniques for EEG signal processing and analysis is shown in Fig. 4. The raw EEG data is processed through these techniques to get the most indicative features. There are various signal processing techniques such as Fourier transform (FT), wavelet transform (WT), empirical mode decomposition (EMD), variational mode decomposition (VMD) and Fourier decomposition method (FDM).

1) PREPROCESSING

When we record an EEG signal, various types of noises and artifacts may occur, which may be reduced by certain preprocessing steps. Following are the several kinds of artifacts that may be observed in EEG recordings.

- Physiological artifact
- Muscle artifact
- External artifact
  - Electrosurgical noise
  - Electrode contact noise
  - Power line interference
  - Noise produced by electronic equipment used in signal acquisition/processing

Physiological artifacts arise due to eyeball movement, eye blinking, and eyelid movement [18]. The presence of physiological artifacts is reflected by the enhanced amplitude of the EEG signal. Muscle artifacts result due to chewing, tongue movement, yawning, and swallowing. The amplitude of the temporal electrode signal changes due to the presence of muscle artifacts. External artifacts occur due to the presence of electronic sources in the vicinity of EEG recording equipment. Movement of the electrode, use of phone, displacement of the electrode, and fluctuation in the power line may be the reason for external artifacts. Numerous filters are used to remove various noises and artifacts [19]. Power line interference is made up of harmonics that may be described as sinusoids of 50 Hz (in India). It does not change the detector analysis. Typical parameters for this are the fundamental frequency with harmonics and peak-to-peak amplitude upto 50%. Electrode contact noise is the transient hindrance engendered due to the least or no contact between the electrode and skin. Typical parameters for electrode contact noise are frequency (50 Hz), amplitude (maximum recorder output), and duration (1 second). Removal of artifacts is performed using manual and automated methods. The manual method indulges the involvement of the technologist to either remove or ignore the artifacts for a particular time slot (when they occur) by inspecting the EEG recording [20] wheres automated artifact removal technique's popular method is Filtering. A single filter is not useful for the removal of all the noises and artifacts due to their occurrence at different frequencies within the entire bandwidth of the EEG signal. Different types of filters are used for different types of artifacts. A high pass filter (HPF) removes high-frequency noises and artifacts such as power line interference [21]. A low pass filter (LPF) extricates DC offset which is engendered due to electrode/electrode gel/body interface. LPF is usually preferred for baseline wander noise removal. Notch filters may also be used to extricate power line interference. Median filters are used to remove outliers and shot noise. Further,

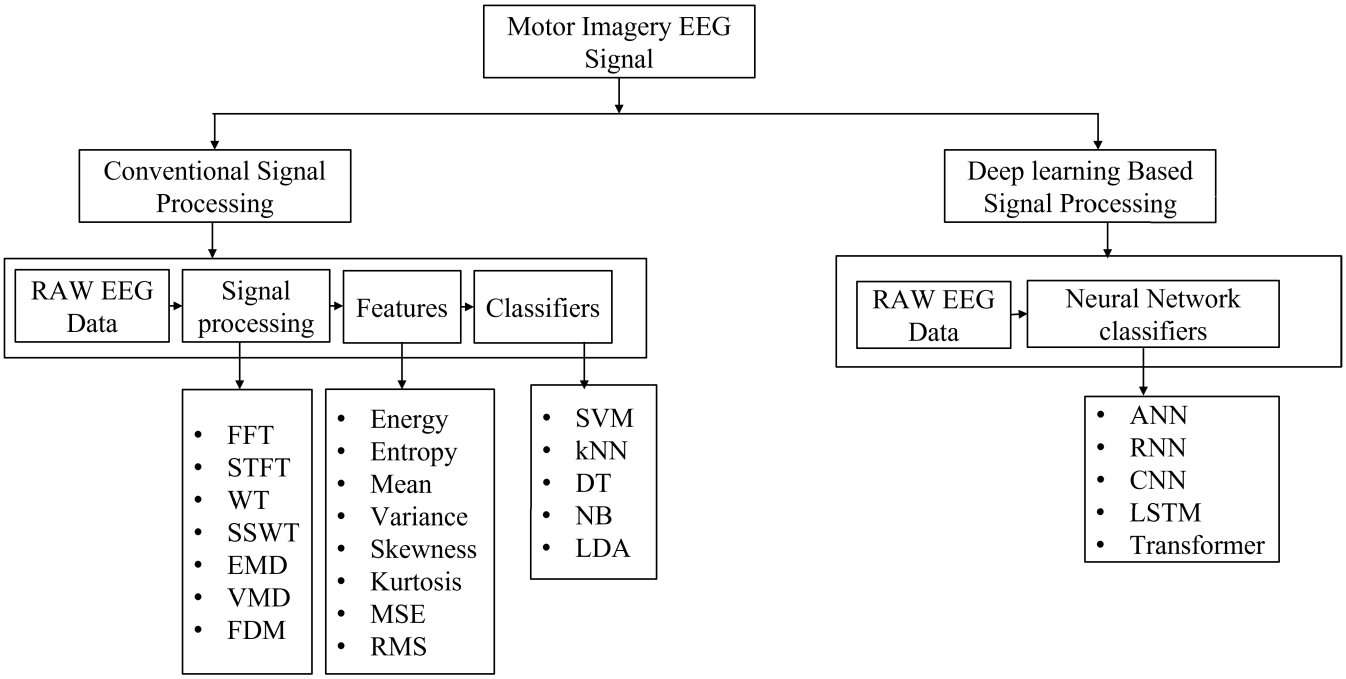

FIGURE 3. The proposed categorization for MI EEG signal analysis.

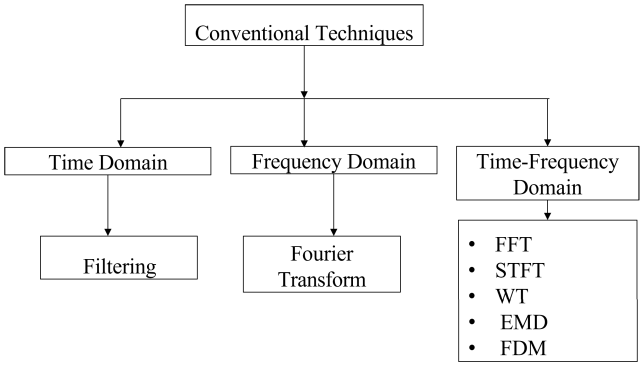

FIGURE 4. Categorization of conventional signal decomposition techniques.

adaptive filters may be considered to remove different types of noise [22].

2) SIGNAL DECOMPOSITION TECHNIQUES

Fourier transform (FT) is employed for the majority of signal processing approaches for stationary signals. FT transforms a time-series vector into frequency domain. Therefore, it is also referred as a frequency-domain method. It produces a complex-valued function, i.e., it includes both magnitude and phase parameters. Fast Fourier transform (FFT) is a fast way to compute the discrete Fourier transform (DFT) or inverse DFT of a signal. The DFT converts a sequence of N real/complex numbers $x[n]$, $0 \leq n < N$, into a different complex number series, $X(k)$, $0 \leq k < N$, can be represented as,

$$X(k) = \sum_{n=0}^{\mathbb{N}-1} x[n] e^{-j2\pi kn/N} \tag{1}$$

FFT works by decomposing the DFT matrix into a product of sparse factors which results in reduced computational complexity. It is used for processing of stationary signals and is befitted to narrowband signals. It possesses some disadvantages, such as, it cannot extract frequency component along with the time information. It cannot analyze the non-stationary signal. This technique is not suitable for extracting spatial information of a signal. It cannot reveal localized spikes and complexes. It suffers from large noise sensitivity [23].

Short-time Fourier transform (STFT) overcomes the disadvantages of FT. As compared to FT, STFT can better deal with non-stationary signals. Here, we divide the signal into a smaller segments and then apply FT to each segment. Here, $x(n)$ is a input signal, $w(n)$ is the window function, then

$$X(k, w) = \sum_{n=0}^{\mathbb{N}-1} x[n] w[n-k] e^{-j\omega n} \tag{2}$$

Here, a chosen finite-length window function is placed first on top of the signal at $t = 0$. Next, the window function is dragged to the right. After this truncation is done until the window approaches the end of the signal. It is quite simple to implement. But it suffers from the limitations of fixed window function and confusing resolution due to which it becomes difficult to differentiate the time of various frequency components [24].

Wavelet transform decomposes the signal into wavelets and also overcomes the disadvantages of STFT. Wavelets are defined by their basis functions. A well-localized function in time and frequency is required for reliable analysis of signals and images with abrupt changes, as these changes cannot be

efficiently analyzed by FT. In this approach, we can change the size and location of the wavelet by scaling and translation of the mother wavelet. Different types of mother wavelets include Haar wavelet, Mexican hat wavelet, biorthogonal wavelet, Gaussian wavelet, and Shannon wavelet [25]. For the purpose of calculating the correlation coefficient, the wavelet under consideration is compared to a segment at the beginning of the original signal. The wavelet is then slided and then the above steps are repeated till completion of the signal. Thereafter, the signal is scaled and all these steps are repeated. If u is scaling factor, v is translating factor, $\psi^*(t)$ is mother wavelet function, the wavelet function $W_\psi(f)$ is represented as

$$W_\psi(f) = X(u,v) = \frac{1}{\sqrt{u}} \int_{-\infty}^{\infty} x(t)\, \Psi^* \left(\frac{(t-v)}{u} \right) dt \quad (3)$$

It provides us a way for analyzing a function in both time and frequency domains. It accurately deconstructs and reconstructs the signal. It can also represent the function that has discontinuities and sharp peaks. But there are also some limitations like oscillations at discontinuity, aliasing, and less effective in capturing directional information [26].

Fourier decomposition method (FDM) [27] provides us with an algorithm, based on Fourier representation, for non-linear and non-stationary data. FDM generates a small set of Fourier intrinsic band-limited functions (FIBFs) [28]. FIBF must fulfill the following criteria:

- It should be a zero-mean function.
- It should be an orthogonal function.
- It should admit the analytic FIBF (AFIBF) representation, i.e.,

$$x_i(t) + j\hat{x}_i(t) = a_i(t)\, exp\left(j\phi_i(t)\right), \quad (4)$$

where $a_i(t)$ and $\phi_i(t)$ denote the instantaneous amplitude and phase, respectively.
The algorithm for low to high-frequency scan (LTH-FS) is:

- Obtain

$$X(k) = FFT\{x[n]\} \quad (5)$$

- Set $AFIBF_i$ as

$$\sum_{k=M_{i-1}+1}^{M_i} X[k]\, e^{j\frac{2\pi kn}{M}} \quad (6)$$

- Acquire the maximum value of M_i such that

$$M_{i-1} + 1 \le M_i \le \frac{M}{2} - 1 \quad (7)$$

- AFIBF phase is a monotonically increasing function, and the instantaneous frequency is

$$\omega_i[n] = \left(\frac{\phi_i[n+1] - \phi_i[n-1]}{2} \right) \ge 0 \quad (8)$$

Synchro-squeezing wavelet transform (SSWT) [29], Empirical mode decomposition (EMD) [30], and Variational mode decomposition [31] are also very popular and robust signal decomposition techniques.

Table 3 provides us the comparison of popular conventional techniques used in the literature.

3) FEATURE EXTRACTION

Some popularly used features are listed below:

Energy represents the strength of a signal to locate series in the power curve at any time [32],

$$E = \sum_{i=1}^{N} \left(x_i^2 \right) \quad (9)$$

where x_i represents samples, E represents energy, and N is the total number of samples.

Entropy is a measurement that assesses the unpredictability of a signal [35] and is calculated as

$$EN = \sum_{i=1}^{N} \left(x_i^2 \right) \log \left(x_i^2 \right). \quad (10)$$

Variance is defined as the mean squared difference between each data point and the center of the distribution represented by the mean [35].

$$\sigma^2 = \frac{1}{N} \sum_{i=1}^{N} (x_i - \bar{x})^2 \quad (11)$$

where $\bar{x}$ represents the mean value and σ^2 represents the variance of the signal.

Measures of central tendency are the mode, median, and mean. The total of all of the scores divided by the total number of scores is the mean (also known as the arithmetic average). The median is the midpoint value in a list that is ordered from the smallest to the largest value. The mode is the value that occurs most frequently in the list [36].

Correlation is the parameter used to analyze the strength of the relationship between the variables that are under consideration [36].

$$R_{XY} = \frac{\sum (x_i - \bar{x})(y_i - \bar{y})}{\sqrt{\sum (x_i - \bar{x})^2 (y_i - \bar{y})^2}} \quad (12)$$

where $\bar{x}$ and $\bar{y}$ represent the mean of two random variables X and Y, respectively, and N is the number of samples, R_{XY} represents the correlation of these two random variables.

Root mean square is the square root of the squared function's mean value [36], i.e.,

$$X_{rms} = \sqrt{\frac{1}{N} \sum_{i=1}^{N} x_i^2}. \quad (13)$$

Maximum minimum distance (MMD) is the distance between the maximum and minimum points [36] and is calculated in the kth sliding window by the Pythagorean formula as:

$$D_k = \sqrt{\Delta x_k^2 + \Delta y_k^2}, \quad (14)$$

TABLE 3. Comparison of transforms.

Transform	Hilbert [32]	Wavelet [33]	Fourier [34]
Basis Frequency	Adaptive	Priori	Priori
Frequency	Convolution: local, certainty	Convolution: regional, uncertainty	Convolution: global, uncertainty
Representation	Time -Energy	Time -Energy	Energy
Nonlinear	Yes	No	No
Non-stationary	Yes	Discrete: No	No
Extracted features	Yes	Continuous: Yes	No
Approach	Empirical	Theory	Theory

where Δx_k and Δy_k are the x-axis and y-axis differences. Total MMD [37], [38] can be obtained by summing over all the sliding windows:

$$MMD = \sum_{k=1}^{N} D_k \tag{15}$$

The log root sum of sequential variation (LRSSV) is a measure of sequence variation between samples of the signal [36]. LRSSV can be calculated as

$$LRSSV = \log_{10} \sqrt{\sum_{n=1}^{N} (x(n) - x(n-1))^2}. \tag{16}$$

Phase mean and phase standard deviation is the measure of angle associated with an analytic signal [37], [38]. The Hilbert transform of the real part of the complex analytical signal is the signal's imaginary component. From the analytical signal $y(t)$, the phase is retrieved, where $y(t)$ is represented as

$$y(t) = x(t) + j\hat{x}(t), \tag{17}$$

with $\hat{x}(t)$ is the Hilbert transform of $x(t)$. $y(t)$ is expressed in polar form as

$$y(t) = A(t)\, e^{j\phi(t)} \tag{18}$$

where $A(t)$ and $\phi(t)$ are magnitude and phase of the analytic signal.

Power spectral density describes the distribution of power amongst frequency components of a time-series [38], i.e.,

$$S_X(f) = \int_{-\infty}^{\infty} R_x(\tau)\, e^{-2j\pi f \tau} d\tau, \tag{19}$$

where $S_X(f)$ represents the FT of the auto-correlation function $R_x(\tau)$. The expected power of $x(t)$ can be obtained by

$$E\left[x^2(t)\right] = R_x(0) = \int_{-\infty}^{\infty} S_x(f)\, df. \tag{20}$$

If X and Y are two random variables, then cross-spectral density is obtained as

$$S_{XY}(f) = \int_{-\infty}^{\infty} R_{xy}(\tau)\, e^{-2j\pi f \tau} d\tau. \tag{21}$$

4) FEATURE DIMENSIONALITY REDUCTION

Algorithms for feature dimension reduction are mentioned below.

Principal component analysis is a statistical procedure, where the first principal component has the highest variance. Successors are chosen with decreasing order of variance but with the condition that the they should be orthogonal to the previous one. Therefore, the resulting vectors form a set of uncorrelated orthogonal basis. Its limitation is that it captures only linear correlations [39].

Linear discriminant analysis optimizes the ratio of within-class variance to class variance. It offers us the best performance in terms of discernment between the various classifications. It is also known as normal discriminant analysis or discriminant function analysis. It is related to regression and variance analysis. LDA seeks to model the difference between the classes of data rather than the similarities between them [40].

Independent component analysis measures multi-dimensional data into features that are statistically independent of each other and exhibit Gaussian character as well [41]. This is an exclusive case of blind source separation (BSS). Independent source signals with non-Gaussian distribution values provide the best results with ICA.

Spatial filtering is a technique for enhancing the signal-to-noise ratio of EEG signals for MI based BCI applications. There are different methods for spatial filtering in MI-EEG BCI, such as common spatial pattern (CSP), filter bank common spatial pattern (FBCSP), and Riemannian transform. The spatial domain is also considered one of the important domains for extracting good features but the main drawback associated with CSP is the need for multichannel information and loss of information in the frequency domain. It allows for identifying components in which the variance in the two classes is most different. Nowadays, researchers are combining CSP with the time domain and frequency domain methods, which undoubtedly provides good results compared to earlier. But still, it suffers from a lot of drawbacks such as settling issues, end effects, and unexplained negative frequencies. Researchers are exploring new variants of CSPs to improve accuracy such as CSP-LDA [42], filterbank CSP (FBCSP) [43], regularized CSP (R-CSP) [44], common spatio CSP (CSSP) [45], common sparse spatio CSP (CSSSP) [46], and sub-band CSP (SBCSP) [47].

5) PATTERN CLASSIFIERS

Once we have the optimal set of features, then we need to investigate different types of classifiers for decision-making. Some of the well-known classifiers are discussed as follows.

Support vector machine (SVM) is one of the foremost and classic algorithms for classifying various data points. Data points, also known as support vectors, are categorized using this method. The kernel function is used to design

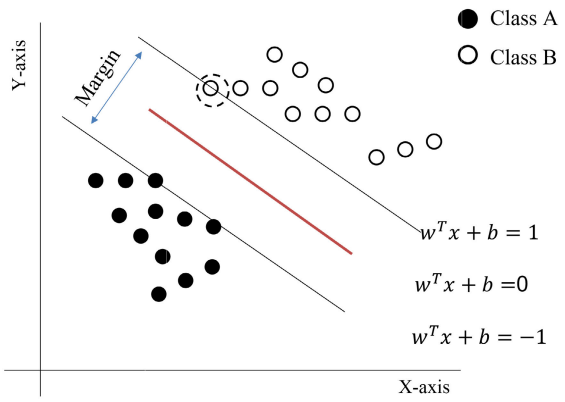

FIGURE 5. SVM for binary classification.

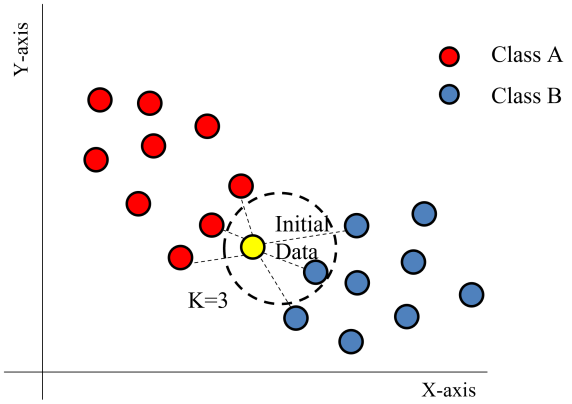

FIGURE 6. Visual representation of kNN Classifier for $k = 3$.

a hyperplane for the support vector. There are many kinds of kernel functions, including radial, polynomial, radial-integral, and linear. A plane that crosses the center of the data points is known as a hyperplane. Its function is to produce the correct separation class for the data set. The maximum margin will be in the region enclosed by the hyperplane. The separating hyperplane and the slab's edge are where support vectors of groups +1 and -1 are located closest as shown in Fig. 5. Using the appropriate techniques for recognizing support vectors, the margin may be increased to the fullest extent [48], [49].

k-nearest neighbor (kNN) is a nonlinear classifier employed in the process of classification. Euclidean and Mahalanobis distance metrics are adopted for achieving the best results. Here, the data points are compared with already trained data sets. The data points are classified by the maximum number of nearest neighbors, with k representing the number of neighbors being compared. Firstly, two-third of the total data is trained, and the remaining one-third is tested for optimal results. The two classes are defined as class A and class B, as shown in Fig. 6. When we need to classify the new data, its distance is measured with neighbors based on the nearness of data, and the calculated distance is compared with the trained data. Then accordingly it is labeled in one class [50].

Artificial neural network (ANN) is a commonly used classifier. A minimum of three layers make up the network which are referred to as input, hidden, and output layers. The primary layer is the input layer which consists of neurons. The hidden layer performs all the data processing consisting of neurons. There may exist more than one hidden layer in a system and the signal's classification outcome is determined by the output layer, which is the final layer. The important parameter involved in the classification of an ANN-based classifier is the activation function and learning rule. The basic structure is shown in Fig. 7. Recurrent ANN is a closed-loop structure ANN that can perform the highly non-linear mapping.There exist some other networks as well [51].

Decision tree (DT) is a classification and regression tool. It uses a tree-like structure, with each node representing for

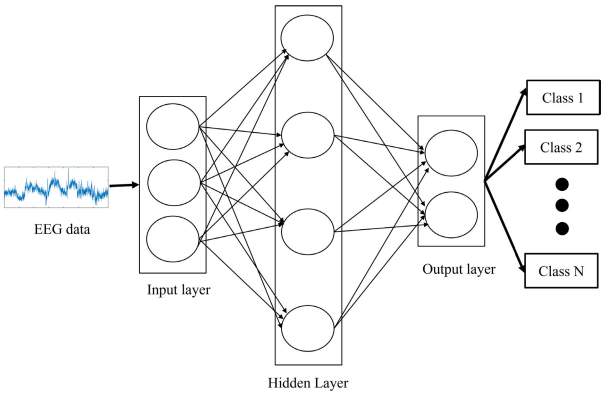

FIGURE 7. ANN classifier for MI EEG classification.

a test performed on the data, and each branch for the test's result. The leaf node denotes the class label of the data as explained in Fig. 8. There are two basic types of algorithms for constructing a decision tree, i.e., iterative dichotomiser 3(ID3) and collection regression tree (CART) [52]. Entropy, information gain and Gini impurity are used as metrics by ID3 and CART [53].

Table 4 provides a comparison of the features and limitations of the above-mentioned classifiers.

B. DEEP LEARNING TECHNIQUES

As the dataset gets bigger it becomes difficult to attain appropriate results with conventional signal processing techniques. However deep learning-based approach works better in such cases. Some deep learning-based approaches have been listed in Fig. 9. These techniques can be used for multiple purposes in BCI data analysis. For the purpose of denoising, restricted Boltzmann machine (RBM), autoencoders and its variants can be used; for data augmentation, variational autoencoder (VAE) and generative adversarial network (GAN) can be used; and for classification, multilayer perceptron (MLP), long short-term memory (LSTM), gated recurrent unit (GRU), bi-LSTM, and convolutional neural network (CNN) can be used.

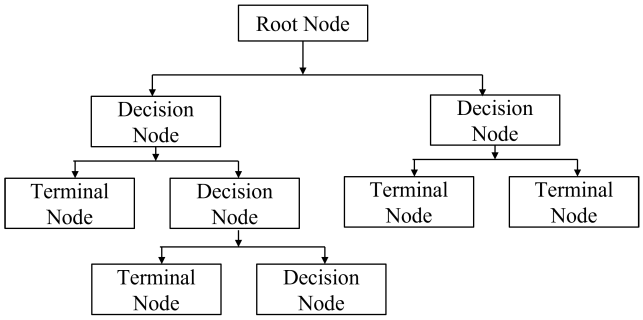

FIGURE 8. Approach of decision tree classifier.

Deep learning-based approaches for MI-EEG signal processing have been categorized as supervised, unsupervised, generative, and hybrid approaches. In the current section, MLP, CNN, recurrent neural network (RNN) and transformers will be discussed for classification under the supervised approaches. Autoencoders (AE) and RBM algorithms are used for denoising and dimensionality reduction under unsupervised approaches. VAE and GAN are used for data augmentation under generative approaches. Hybrid approach is a combination of supervised and unsupervised approaches, supervised and generative approaches, and unsupervised and generative approaches.

1) SUPERVISED APPROACH

Supervised algorithms require the training dataset which contains input MI-EEG data with its classification label. The training of these supervised algorithms requires following steps:

- Algorithm will take the pre-processed MI-EEG as input.
- These signals are passed though model to extract features.
- These features help in getting classification predicted output probability vector by SoftMax layer.
- Compare the predicted output vector from the desired label and calculate the loss.
- Gradient of loss is back-propagated to update the model parameters.
- Repeat steps 2 to 5 until the loss converges.
- After loss convergence, one can use trained model to compute the accuracy on testing dataset.

We now discuss the models that have been used for bio-medical classification tasks.

MLP has been used for classification for biomedical signals in [54]. It has input and output layers along with hidden layers as shown in Fig. 10. An arbitrary activation function is used for imposing a threshold. Activation functions decide whether neurons should be fired or not. The major limitations associated with MLP are gradient diminishing problem [55], long training time on large data set, and the converging loss is not optimal. These issues hinder the classification performance on MI-EEG signal classification and processing.

CNN: It is an eminent dense neural network architecture that performs the convolutional operation. CNN architectures are used by [56]for binary and multiclass classification for MI EEG signals. This network can work on images [57], audios [58], videos [59] and EEG as specific signal [60]. Its architecture comprises the input layer, a combination of convolution and pooling layers, a fully connected layer, and an output layer. Convolution helps in extracting high-level features. A deeper network suffers from a problem of overfitting though it can be resolved easily by using ReLU as an activation function [61]. The basic architecture of CNN is shown in Fig. 11.

The important parameters of CNN are kernels, stride, padding, pooling, and flattening. A **kernel** is a matrix that slides by stride value over the data and executes the dot product with the sub-region of data and gets the dot product matrix as output. It is a sort of filter which extracts features from images. **Stride** is the amount with which kernel slides over data. It is symmetrical in height and width dimensions. A kernel is passed across the image towards the right hand and then top to bottom with pixel column and row change in horizontal and vertical movements. **Padding** is the best technique where convolutional kernel pixels are needed for processing edge pixels. Generally, padding of zeros is added at the edge of the image. It also solves the problem of the border effect. With the preservation of significant characteristics, **pooling** is employed to reduce the dimensionality. The maximum value is chosen during pooling, which is known as max pooling. Min pooling is one option where the minimum value is picked. The average value may be selected via average pooling. **Flattening** is the last step where the entire feature matrix is converted into a column or row vector. Later, this vector is fed to a fully connected layer, followed by SoftMax layer.

RNN is used for time-series data. It plays a vital role in extracting features from sequential data. In RNN, output of each neuron depends upon its input and previous output of that neuron and this feedback works as a memory unit [62]. RNN has the problem of exploding and vanishing gradients [63]. These problems may be resolved by using three advance variants of RNN [61], [62]: LSTM, GRU, and bi-LSTM.

LSTM model comprises three gates: The input gate, forget gate, and the output gate, as shown in Fig. 12. Unlike RNN, it can work in both directions to form unidirectional and bidirectional LSTM [64]. LSTMs work as a building block for deep RNN architecture [62]. It can read, write, and delete information from memory. Memory is used as a gated cell that decides to allow new input in (input gate), eliminate or keep the data by observing its importance (forget gate), and check the impact of output (Output gate). LSTM learns its weights with time to segregate the information that is needed.

GRU is a current generation of RNN. In comparison to LSTM, it has a reset gate and an update gate [65]. There is no cell state in GRU, only a hidden layer is used for transferring information. Here, reset gate concludes which past data to

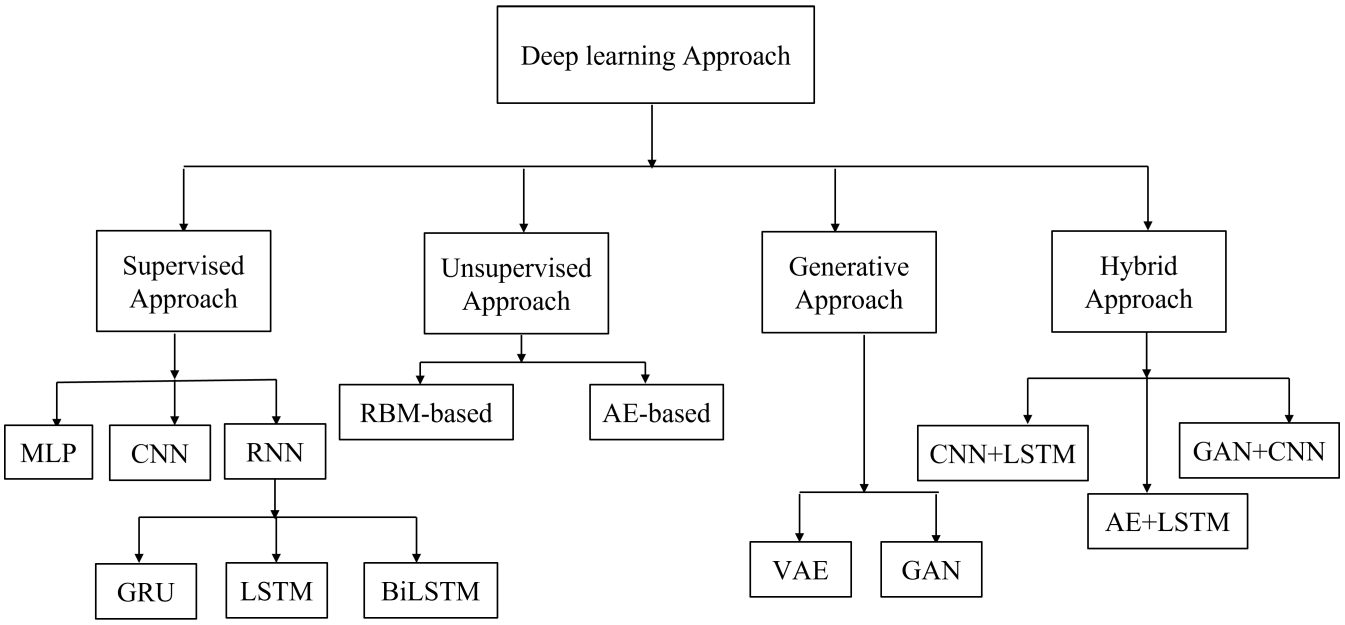

FIGURE 9. Classification of deep learning signal processing techniques for MI EEG signals.

TABLE 4. Comparison of classifiers.

Algorithm	Features	Limitation
Support vector machine algorithm	It works well even if data is not linearly separable	For testing and training purposes it requires more speed and size
(SVM) [48]	It stipulates high accuracy to us.	It requires high complexity and memory for classification purposes
k-nearest neighbor algorithm	It is well delineated for multimodal classes.	Its performance depends upon several dimensions we use in the dataset.
(KNN) [50]	It has zero cost for training. Unlike SVM it is subtle if data is not linearly distinguishable. It is vigorous to noisy data.	Its performance depends upon several dimensions we use inthe dataset. It is very delicate to noise and irrelevant features. It takes a huge amount of time for the larger dataset
Artificial neural network algorithm (ANN) [51]	It applies to a wide range of applications Unlike SVM it is subtle if data is not linearly distinguishable. It is vigorous to noisy data.	Its learning can be slow.
	It is easy to implement.	It takes a long time for a large data set.
	Once it is trained then there is no need of reprogramming it.	We cannot predict how many neurons and layers are to be needed.
	Once change parameters, it is quite easy to use this.	
Decision tree (DT) [53]	It provides good accuracy.	It needs large memory to store the decision tree.
	Its detection rate is less.	Sometimes rules are extensive to prune.
	Its space consumption requirement is less.	Its searching period is high.

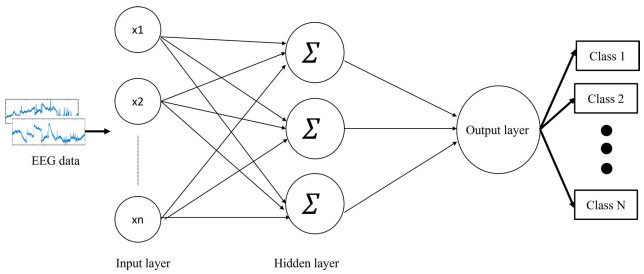

FIGURE 10. Architecture of multilayer perceptron (MLP) for classification.

forget and the update gate decides which data to forget and add to the reset gate. The basic GRU block is shown in Fig. 13.

Bi-LSTM architecture is generated by keeping two independent RNNs together as shown in Fig. 14. It gives us the benefit of transferring information in both backward and forward directions, unlike other RNNs. This type of RNN has been successfully implemented on speech data. This input is fed in an unusual way that is one from past to future and the other is from future to past [66].

Transformer processes sequential data and its architecture includes encoder and decoder like other neural network architecture as shown in Fig. 15 [67]. Input provided in encoder is a combination of input embedding and positional information. Positional information is necessary for proper sequence of data. Encoder consists of self-attention and feed

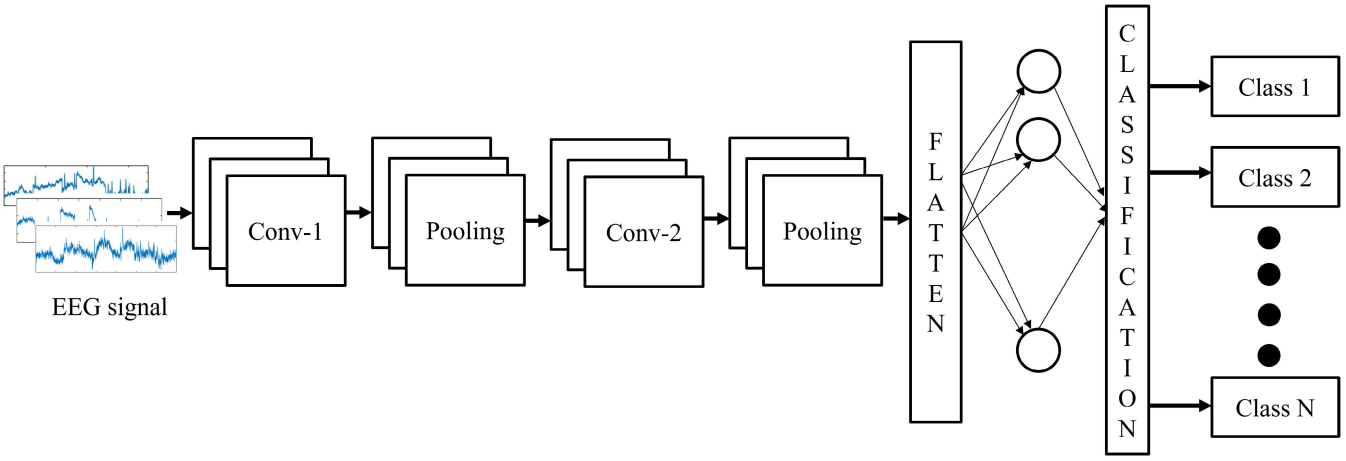

FIGURE 11. CNN Model for classification.

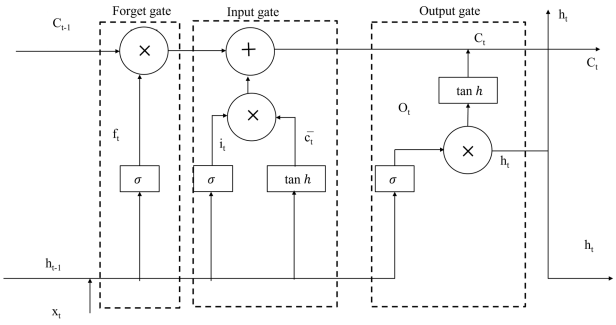

FIGURE 12. Architecture of a block of LSTM for classification.

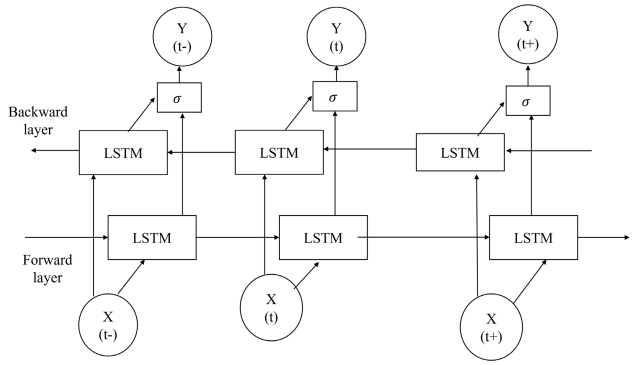

FIGURE 14. Architecture of a block of Bi-LSTM for classification.

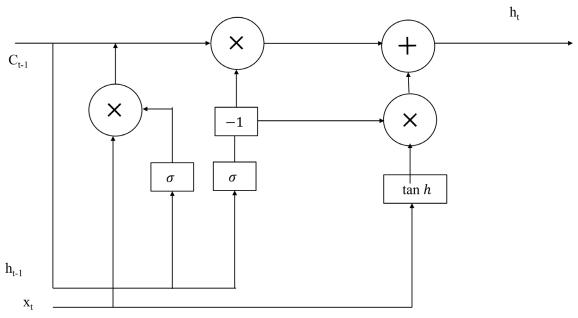

FIGURE 13. The GRU for classification.

forward network whereas decoder has one more layer of encoder-decoder attention due to which relevant information generated at encoding is used in decoder. Transformer uses a similarity function of scaled dot product that learns from three weight matrices of query(Q), key(K), and value(V) whose dimensions are d_q, d_k, d_v. One set of attention (w_q, w_k, w_v) is called head and the layer with all the sets of attention is called multi head attention layer. The fast processing of transformer is due to parallel computation of each attention head. All heads are concatenated and transformed using square weight matrix. Attention weights are calculated using query and key. These weights are divided by square root of dimension of key vector for stabilizing gradient. Finally, this is passed to a SoftMax function for normalization.

2) UNSUPERVISED APPROACH

Unsupervised algorithms are used for bio-medical signal denoising and dimensionality reduction [66]. There are following deep learning based unsupervised algorithms which are commonly used for MI-EEG data.

RBM: The Boltzmann distribution is the basic phenomenon behind this denoising algorithm. It is also named Gibbs distribution. Boltzmann machines are generative deep-learning models which are non-deterministic (or stochastic) [68]. RBMs are two-layered neural networks that belong to a class of energy-based models that can detect inherent patterns in data automatically by reconstructing clean signal from noisy input. These functioning blocks are the hidden layer and the visible layer, as shown in Fig. 16. It does not have any output layer. When the input is fed, they encapsulate every feature and compute correlation among the data. The presence of only two layers makes it different from autoencoders. A hidden layer activation function is active and passed to the visible layer for the reconstruction of the signal. They cannot transfer information among themselves as generated signal differs from the input signal. RBM is a

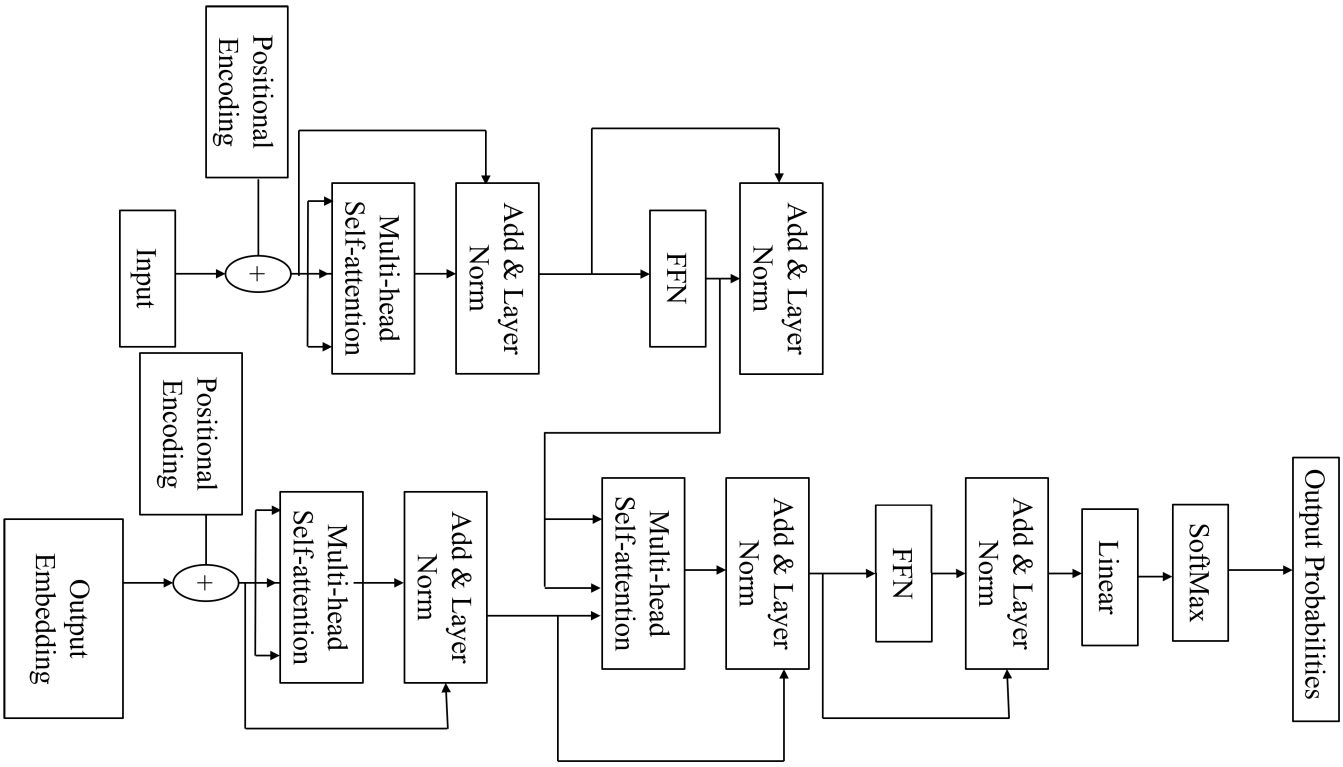

FIGURE 15. Architecture of transformer for classification.

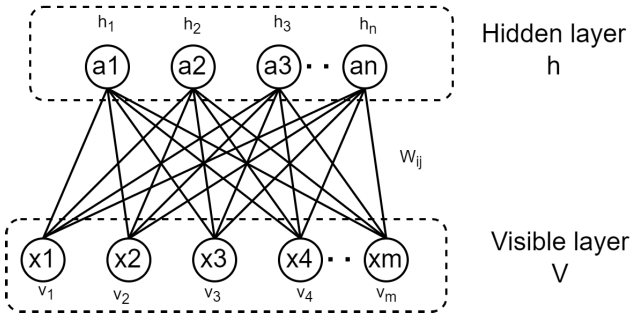

FIGURE 16. Architecture of RBM for denoising.

non-deterministic network where each neuron behaves randomly at activation.

Autoencoder is a representative artificial neural network (ANN) technique that learns to compress and encode data efficiently [69]. Later, it perceives how to regenerate data back from the reduced encoded representation. This newly generated data should be very much like the original input. It is an incredibly good denoising technique. Its functioning blocks are encoder, latent space, and decoder. An encoder is used to reduce the dimensionality of noisy MI-EEG data (data with noise) whereas a decoder regenerates the input data as output of the decoder. Code is a dense precise input which is called latent space representation. It is a flatten layer of any dimensionality whose nodes in the layer (code size) act as a hyperparameter that we set before training the autoencoder. Input is fed to the encoder which helps in generating code. Here decoder is a mirror image of the encoder. The aim is to get the denoised output from the noisy input. Fig. 17 shows the basic architecture of autoencoder for denoising. These hyperparameters should be set before training an autoencoder:

- Code size: For reduced dimensionality, smaller size of code is needed. It is the number of nodes in the middle layer.
- Number of layers: like any other ANN there could be any number of layers for the encoder and decoder
- Number of nodes per layer: There can be any number of nodes for each layer. As the decoder is a mirror image of the encoder so it should keep the same layer structure as the autoencoder.
- Optimization function: Mean squared error (MSE) and cross-entropy are the most common parameters used for the calculation of optimization function. If the input values are binary then we use cross-entropy, otherwise, we use the mean squared error. The loss is computed between reconstructed output and clean MI-EEG input.
- Backpropagation algorithm is used to update the weights of encoder and decoder by optimizing the loss function.

3) GENERATIVE APPROACH

VAE is an autoencoder whose training is normalized for avoiding overfitting and setting up the latent space for an efficient encoding process [70]. It consists of an encoder and decoder just like other autoencoders as shown in Fig. 18.

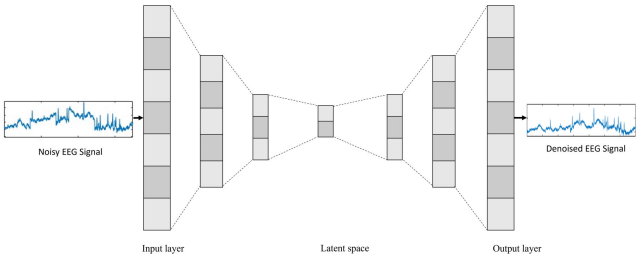

FIGURE 17. Architecture of autoencoders for denoising.

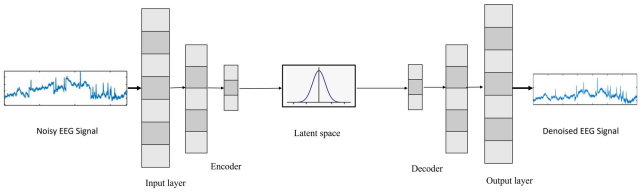

FIGURE 18. Architecture of variational autoencoders for denoising.

Moreover, we can say that it is regularised version of autoencoders. Along with this, it also considers loss function which makes this different from autoencoders. VAE solves the concern of the indiscretion in latent space by doing distribution all over the latent space despite a single point, and then for better orderliness of the latent space, the loss function is added for regularization. Regularisation is made of two properties; one is continuity, and the other is completeness. The encoder has input distributed over the latent space. Later, points from that latent space will be sampled and fed to the decoder. From the output of the decoder, reconstruction loss is computed and back-propagated. But there is a trade-off between reconstruction error and regularization [70].

GAN consists of two major parts named as generator and discriminator [71]. In the generator, any random data from known distribution is provided as input to generate real data synthetically. Then, the discriminator tells whether the generated sample is real or fake. The output of the discriminator remains binary where 1 refers to real data and 0 refers to the fake data. Discriminator knows that how real data looks like. This network has generator loss (mean square error, VGG loss etc.) as well as discriminator loss (cross-entropy). The weight of generator is updated by optimizing generator as well as discriminator loss. The optimization function is formulated as a min-max problem where the generator tries to maximize the total loss and the discriminator tries to minimize the discriminator error. We optimize the loss until an equilibrium stage is reached, where the discriminator becomes confused in classifying the generated output as real or fake. Equation (23) shows min-max loss equation where the probability that the generator correctly classifies the actual data is $log(D(x))$ and increasing $log(1 - D(G(z)))$ would make it easier for the discriminator to identify the false picture produced by the generator. $D(x)$ is real data probability estimation of discriminator, $G(z)$ is generator output, D(G(z)) is fake probability estimation of discriminator, E_x is expected value of real data, and E_z is expected value of all data given to generator. Fig. 19

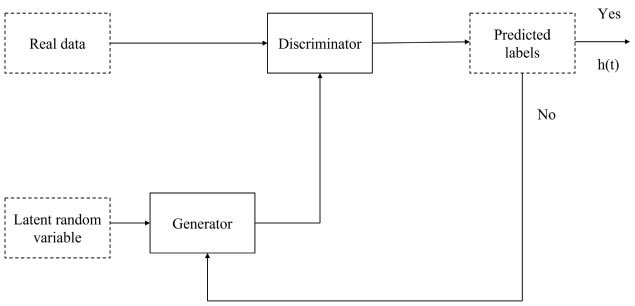

FIGURE 19. Architecture of Generative adversarial network (GAN) for data augmentation.

shows the basic architecture of GAN. It is used by [72] to generate bio-medical signals to boost classification accuracy.

$$E_x\left[\log\left(D\left(x\right)\right)\right] + E_z\left[\log\left(1 - D\left(G\left(z\right)\right)\right)\right] \quad (22)$$

4) HYBRID APPROACH

Hybrid algorithm is a combination of different types of supervised and unsupervised approaches, supervised and generative approaches, and unsupervised and generative approaches [73]. Recently, researchers have combined CNN with LSTM [74], autoencoders with LSTM [75], and CNN with GAN [76] to extract more efficient features. These hybrid algorithms are providing good performance. Table 5 provides us the comparison of deep learning based techniques used in literature.

III. DATASETS

Many datasets have been in use for the study of various techniques and analysis of Motor imagery signals. The number of individuals, number of electrodes, trial length, total number of trials, sampling frequency, and the number and types of MI tasks vary from dataset to dataset. The largest collection of data is available at:

- Physionet dataset is collected from 109 subjects with 64 electrodes. There is only 1 session with 270 trials of 10 seconds. The sampling frequency is 160Hz [77].
- High Gamma dataset is collected from 14 subjects with 128 electrodes. There is a total of 13 sessions with 1000 trails of 4 seconds [78].
- BCI competition dataset is popular among researchers. BCI-C IV 2a and 2b datasets are benchmark for EEG based motor imagery signal classification. Its various sub-parts include a diverse number of subjects, trials, and electrodes for a description of the MI task [79], [80].

The description of all the BCI datasets is provided in Table 6.

IV. PERFORMANCE MEASURES

Various performance measures help us in evaluating the system performance. True Positive (TP) refers to accurate identification of a condition or trait while False Positive (FP) refers to incorrect identification of a condition or trait. True Negative (TN) refers to accurate identification of the

absence of a condition or trait whereas False Negative (FN) denotes incorrect identification of the absence of a condition or trait [81], [82], [83], Various performance measure can be defined Using TP, TN, FP and FN. Few of them are defined as:

Accuracy is the ratio of sum of TP and TN with the total number of samples in dataset i.e.,

$$Accuracy = \frac{TP + TN}{TP + TN + FP + FN}. \tag{23}$$

Specificity is the ratio of actual negative samples to the number of total negative predicted samples. It is computed as

$$Specificity = \frac{TN}{TN + FP}. \tag{24}$$

Sensitivity is determined by the proportion of expected positive samples to actual positive samples, i.e.,

$$Sensitivity = \frac{TP}{TP + FN}. \tag{25}$$

Precision is the ratio of actual positive samples to the number of total positive predicted samples. It is obtained as

$$Precision = \frac{TP}{TP + FP}. \tag{26}$$

F-measure is the harmonic mean between precision and sensitivity.

$$F - measure = \frac{2TP}{FN + FP + 2TP}. \tag{27}$$

Mathew's correlation coefficient (MCC) measures the correlation between actual and predicted class where +1 shows perfect prediction, 0 shows arbitrary prediction and -1 shows perfect conflict.

$$MCC = \frac{TP - FP}{\sqrt{(TP + FP)(TP + FN)(TN + FP)(TN + FN)}}. \tag{28}$$

Receiver operating characteristics (ROC) is a curve plotted between true positive rate and false-positive rate. AUC is the area under this curve [84].

Confusion Matrix is an P matrix for evaluating the performance of a model where P defines several target classes associated with the model. Here, actual values are compared with predicted values. High TP and TN rates and low FP and FN rates are indicators of a good model [85]. Fig. 20 shows the arrangement of confusion matrix.

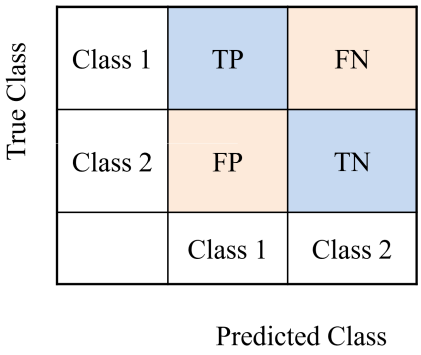

FIGURE 20. Confusion matrix.

V. COMPARISON OF MI SIGNAL CLASSIFICATION TECHNIQUES

This section provides a comparison of conventional and deep learning techniques based on their input formulation, classifier, and performance measure. In section V-A, conventional methods are explained, and in section V-B, deep learning methods are discussed.

A. CONVENTIONAL SIGNAL PROCESSING TECHNIQUES

Kevric and Subasi [86] employed three well-known signal decomposition methods, including wavelet packet decomposition (WPD), DWT, and EMD. The multiscale PCA is used as a denoising approach and higher-order statistical features collectively perform extraction from WPD sub-bands resulting in the highest average classification accuracy of 92.8% amongst these three techniques. However, by using feature selection algorithms, optimal features could have attained with less computation time. Gupta et al. [87] suggested the flexible analytic wavelet transform (FAWT) method for categorizing various MI activities using EEG signals. They achieved an accuracy of 99.33%, sensitivity of 99%, specificity of 99.6%, F1-Score of 0.9925, and kappa value of 0.9865, using time domain-based features and kNN classifier. In [88], slow cortical potentials (SCPs) were analyzed using the wavelet packet analysis (WPA). Using log energy entropy, the output of WPA is further examined, and the resulting feature vectors are passed to MLP for classification. On the datasets Ia and Ib, they reported classification accuracy values of 92.8% and 63.3%, respectively. Taran et al. [89] proposed the analytic intrinsic mode functions (IMF) based features for classification. EMD and Hilbert transform collectively provide IMFs and passed to a least squares SVM (LS-SVM) classifier. The performance parameters included classification accuracy of 97.56%, sensitivity of 96.45%, specificity of 98.96%, a positive predicted value of 99.2%, a negative predictive value of 95.2%, and minimum error rate detection of 4.28%.

Bhattacharyya et al. [90] suggested the use of Fourier-Bessel series expansion (FBSE) to improve empirical wavelet transform (EWT). Signals were segregated into narrow-band components using wavelet-based filter banks, and then the normalized Hilbert transform was employed to evaluate the amplitude envelope and instantaneous frequency functions. The MSE value of multicomponent FM signal for different cases for FBSE-EWT was obtained as 0.0015. Zhou et al. [91] offered an innovative technique based on wavelet envelope analysis and LSTM classifier. HT and DWT were used collectively to extract information on both amplitude and frequency characteristics. Then, the wavelet envelope features were fed to LSTM to achieve a classification accuracy of 91.43%.

TABLE 5. Comparison of deep learning approaches.

Supervised Learning	Unsupervised Learning	Generative Learning	Hybrid Learning
Requires labeled data	Requires unlabeled data	Requires unlabeled data	Requires labeled and/or unlabeled data
Learns to map the input to the output	Learns to discover patterns in the input	Learns to generate new data similar to the input	Learns to combine different objectives or paradigms
Minimizes a loss function based on labels	Minimizes a loss function based on data structure	Minimizes a loss function based on data distribution	Minimizes a loss function based on multiple criteria
Suitable for prediction or inference tasks	Suitable for exploration or analysis tasks	Suitable for synthesis or creation tasks	Suitable for complex or challenging tasks

TABLE 6. BCI competition datasets, where the MI tasks include left hand(LH), right hand (RH), foot/feet (FT), tongue (T), left fist (LF), right fist (RF), both fists (BF), left leg (LL), right leg (RL), both foot (BFT).

Dataset	Channels	No. of subjects	class	Sampling Rate (Hz)
Datasets 1	64	7	2(LH+RH)	1000
Datasets 2a	22	9	4(LH+RH +T+FT)	250
Datasets 2b	3	9	2(LH+RH)	250
Datasets 3	10	2	4(Wrist movement in all four directions)	400
Datasets 4	48-64	3	5(movement of all fingers thumb)	1000
Datasets I	64	1	2(left pinky+T)	1000
Datasets II	64	2	Spell word	240
Datasets IIIa	60	4	4(LH+RH +T+FT)	250
Datasets IIIb	2	3	2(LH+RH)	125
Datasets IVa	118	5	2(Foot+RH)	1000
Datasets IVb	118	2	2(LH+FT)	1000
Datasets IVc	118	1	3(LH+FT+relax)	1000
Datasets V	32	3	3(LH+RH+Word Association)	512

Khalaf et al. [92] employed a common spatial pattern (CSP) algorithms and multi-scale analysis to extract features from fTCD and EEG. Moreover, the Bayesian approach was proposed for the probabilistic fusion of EEG and fTCD despite concatenation. The suggested technique produced results with average accuracy of 93.85%, and average information transfer rate of 19.89 bits/min. In [93], DWT was used to decompose the signal into narrow-band signals which are further decomposed using EMD. From the signal components thus obtained, approximative entropy was computed for classification using the SVM technique. Ganorkar and Raut [94] used wavelet decomposition along with SVM classifier. They used different wavelets and kernels to attain an accuracy of 82.1%. An innovative approach with phase space representation (PSR) and EMD was introduced by Bagh et al. [95]. PSR was applied to the chosen IMFs, obtained using EMD. One-way analysis of variance (ANOVA) test was used to select significant features that were input into several classifiers such as SVM, logistic regression (LR), and Naive Bayes (NB). The SVM classifier reported accuracy of 96.67%, Kappa value of 0.93, and AUC as 0.96.

The characteristics of functional brain networks were combined with CSP and local characteristic-scale decomposition (LCD) features to create a unique approach for retrieving discriminative features in [96]. Extracted features were fused with frequency and spatial domain features which attained average classification accuracy of 79.7%. PCA and FLD (Fisher's linear discriminant)-based Hybrid-KELM (kernel extreme learning machine) methodology were presented in [97]. This method achieved a classification accuracy of 96.54%. For dimensionality reduction, PCA was employed. The FLD presented for an attribute that is far afield of the distinct modules. Wang et al. [98] investigated a hybrid BCI based on motor imagery and speech imagery. All the extracted eigenvalues of CSP, phase-locking value (PLV), and cross-correlation function were combined in synchronization. The three mental tasks with the highest average categorization accuracy were speech imagery (74.3%), left hand motor imagery (71.4%), and right-hand motor imagery (69.8%). Decomposition of signals using the EWT was used by Sadiq et al. [99] to improve MI-based EEG signals classification accuracy. For each channel, a single mode was chosen using the Welch PSD analysis approach, and Hilbert transform method was utilized to extract the instantaneous amplitude (IA) and instantaneous frequency (IF) signal components for each chosen mode. For IA and IF component characteristics, the LS-SVM classifier achieved an average classification accuracy of 95.2% and 94.6%, respectively. In [100], LSTM model with CNN was proposed along with CSP for extracting spatial and temporal features. The kappa value of 0.80 and the classification accuracy of 83% was attained by this method. Chaudhary et al. [101] considered the FAWT decomposition technique to extract time domain-based features from the sub-bands. Using the ensemble learning approach, the subspace kNN classifier provided accuracy, sensitivity, specificity, F1-Score, and kappa values of 99.33%, 99%, 99.6%, 0.9925, and 0.9865, respectively. In [102], the concept of spectro-temporal filtering during pre-processing was proposed where MI-elicited neural patterns are obtained with varying amplitude modulation variations according to artifacts. A two-step classification method was used where firstly, LDA discriminates between different pair-wise MI tasks, and secondly, a naive Bayes classifier foresees the final task to achieve the desired classification.

Kumal et al. [103] proposed hybridization of the oscillatory modes decomposition features mining based on the

second order difference plots (SODPs) of oscillatory modes using EMD and VMD. In this work, Wilcoxon statistical test was used for dimensionality reduction, and machine-learning algorithms were devised to effectively identify alcoholism. For classification, kNN, random forest (RF), LS-SVM, and MLPNN classifiers were employed. The results were noteworthy for MLPNN with 99.89%. CWT and a simplified CNN (SCNN) was proposed in [104] for improving the recognition rate of MI-EEG signals. An image was produced as a time-frequency representation obtained using CWT. These signals were then supplied to SCNN for feature extraction and classification. The mean kappa value was 0.651, and the average classification accuracy among the nine patients was 83.2%. In [105], an ensemble SVM-based voting system was proposed. FT, EMD, discrete cosine transforms (DCT), and CSP based representation of EEG signal was used for each line of this system, which was combined in a triple frame matrix. Then, features were extracted using a pre-trained deep CNN. SVM achieved an average classification accuracy of 96.34%.

Echtioui et al. [106] proposed an architecture with ANN, CNN1, CNN2, CNN1 with CNN2 merged, and the modified CNN1 with CNN2 merged. These methods used different temporal and spatial characteristics of the signal as features. Here, the CNN1-based method achieved a classification accuracy of 68.77%. Authors in [107] used cross-correlation, band power, and Haar wavelet energy (HWE) feature extraction techniques for getting the feature set from the EEG signals. The features were classified using NB, DT, LDA, and QDA. With various classifiers, the achieved accuracy were 92.50%, 93.1%, 72.26%, and 98.71%, respectively. Features were extracted using Lp norms by the FDM method in [108]. The signal was decomposed into a finite number of FIBFs and then relevant features were selected using the Kruskal-Wallis test. Thereafter, SVM was employed to classify the signal. Average classification accuracy of 99.99%, sensitivity of 100%, and specificity of 99.99% were obtained for the binary classification of EEG signals. Authors in [109] proposed the XGBO method to decrease the dimensionality of features while improving accuracy. The MI-based BCI systems' accuracy was increased by this approach by choosing the fewest possible features. This method produced classification errors of 5.56% and 11.28% and mean accuracies of 94.44% and 88.72%. A fusion network was proposed in [110] by combining the features calculated by EMD and ICA. Thereafter, the features were merged in the fully connected layer of CNN, providing an average accuracy of 83.97%.

The comparison of different conventional signal processing techniques based on their techniques used, classifiers used, and performance measures, is provided in Table 7. The accuracy values reported here are taken directly from the published works of the respective authors. Fig. 21 shows the input formulation considered by researchers for analysis of MI EEG data. To the best of our knowledge, we can conclude that about one-third researchers use raw EEG signal whereas rest use spatial domain features and time-frequency domain features. Some of them have transformed signal data into images.

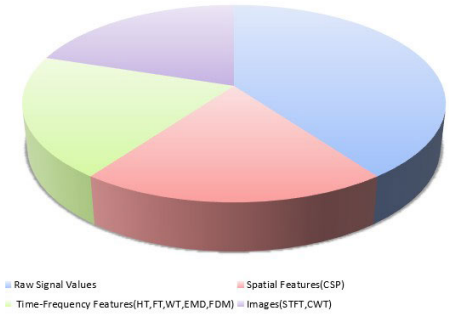

FIGURE 21. Pie chart highlighting the proportions of different input formulations used in the literature.

B. DEEP LEARNING TECHNIQUES

Tabar and Halici [111] proposed a method combining input of frequency, time, and location information from EEG signal in 1D CNN and max-pooling layer with SAE as a classifier. The kappa value achieved by the suggested technique was 0.547. Deep ConvNet decoding performance could be enhanced in [112] by developing batch normalization and exponential linear units together with a trimmed training technique and the FBCSP algorithm. Spectral power modulations in the EEG increased awareness of ConvNets. The proposed algorithm attained satisfactory results with mean decoding accuracy of 82.1% for FBCSP and 84% in deep ConvNets. Sakhavi et al. [113] provided a representation of upgrading the FBCSP approach through the design and optimization of CNN in accordance with the representation. The effective signal representations for LSTM networks with the CSP was derived in [114] using the one dimension-aggregate approximation (1d-AX). This framework's efficacy was increased by the channel weighting approach, which yielded an accuracy of 71%. Authors in [115] outlined a method in which FBCSP algorithm produced spatial features, which were then input into an RNN for classification using cropped time slices of the signals. To combat memory distractions, the RNN design was modified to incorporate the widely used GRU and LSTM unit. The suggested approach offered a fresh approach to build a model robustness and high accuracy. Lawhern et al. [116] introduced a CNN for EEG-based intra-subject and inter-subject classification using BCI paradigms: sensory-motor rhythms (SMR), error-related negativity responses (ERN), P300 visual evoked potentials, and movement-related cortical potentials (MRCP), which achieved comparably higher performance. Two different GDL models were used in [117] to generate an efficient model for the recognition of MI signals, and achieved a classification accuracy of 71%.

Ortiz-Echeverri et al. [118] proposed the combination of a blind source separation (BSS) to obtain estimated independent components, where these components were represented in 2D and classified using CNN. The estimated sources were sorted by BSS using a criteria based on the spectral correlation with a movement related independent component

TABLE 7. Performance comparison of signal processing techniques.

Sr.no.	Author (Year)	Technique	Classifier	Dataset	Accuracy (%)
1	Kevric, J. et al. (2017)	MSPCA+DWT MSPCA+WPD MSPCA+EMD	SVM	BCI III IVa	92.8
2	Gupta et al. (2017)	FAWT	kNN	Bern Barcelona database	99.3
3	Göksu et al. (2018)	WPA	MLP	Private	92.8
4	Taran et al. (2018)	EMD	LS-SVM	BCI III IVa	97.56
5	Bhattacharyya et al. (2018)	EWT+HT	-	Private	-
6	Zhou et al. (2018)	DWT	LSTM	BCI III	91.43
7	Khalaf et al. (2019)	Bayesian+CSP			93.85
8	Ji et al. (2019)	DWT+EMD	SVM	BCI 2b	95.1
9	Ganorkar et al. (2019)	WT	SVM	Intelligent Data Analysis Group, Berlin	82.1
10	Bagh et al. (2019)	PSR+EMD	SVM	–	96.67
11	Ai et al. (2019)	CSP+LCD	_	Private	79.7
12	Venkatachalam et al. (2019)	H_KELM+PCA	_	BCI III	96.54
13	Wang et al. (2019)	CSP+PLV	SVM	Private	74, 3
14	Li et al. (2019)	EWT+WPD	LS-SVM		95.2
15	Zhang et al. (2019)	CNN	LSTM	BCI IV 2a	83
16	Chaudhary et al. (2020)	FAWT	KNN	BCI IV 2a	99, 33
17	Eliana et al. (2020)	LDA	Naïve Bayes	BCI IV 2a	77, 16
18	Li et al. (2020)	CWT+SCNN	SVM	BCI IV 2b	83.2
19	Taheri et al. (2020)	DCT+CSP	SVM	BCI III Iva	96.34
20	Echtioui et al. (2021)	WPD	LSTM	BCI 2a	68.77
21	Roy et al. (2021)	HWE, Band power	DT	BCI III Iva	98.71
22	Thenmozhi et al. (2022)	XGBO	_	BCI IV 2a BCI III a	88.7 94.4
23	Geng et al. (2022)	EMD	CNN	BCI IV 2a	

(MRIC) in order to minimize the spatial variation. By utilizing k-fold cross-validation, the suggested approach was able to attain a classification accuracy of 94.66%. In [119], CSP and the Riemannian geometry feature extraction methods were proposed. The authors have also discussed wrapper feature-selection algorithms, particle swarm optimization (PSO) techniques, and DT classifier was used. Features of the power spectrum density with covariance matrices were projected onto the tangent space. Chaudhary et al. [120] changed EEG signals into images using STFT and CWT, and fed them to the DCNN. AlexNet was employed for classification to obtain a 99.35% accuracy. Using amplitude-perturbation data augmentation and the channel-projection mixed-scale CNN (CP-Mixed Net), an end-to-end EEG decoding framework was suggested in [121]. Primary spatial and temporal representations from EEG data were specifically intended to be learned by the first block in CP-Mixed Net. The classification block was constructed to classify EEG tasks that depend upon the features extracted from CNN. The competitive results demonstrated that the proposed method provided a classification accuracy of 74.6% and 93.75% for BCI and HGD datasets, respectively. Tayeb et al. [122] built three deep learning models using a RCNN, a spectrogram-based CNN, and LSTM. In all the three models, CNN achieved maximum accuracy of 92.28%.

In [123], EEG waves were transformed into a series of a 2D array, preserving the spatial distribution of sampling electrodes, to create the 3D representation. The multi-branch structure demonstrated potent capacity to mitigate overfitting problems with its low latency. The proposed framework's kappa coefficient was 0.64. Xu et al. [124] suggested a framework that consists of a target CNN model that has the same structure as VGG-16 with the exception of the SoftMax output layer, and a VGG-16 CNN model that has already been trained on ImageNet. The target CNN model received the pre-trained VGG-16 CNN model parameters directly. Following that, the target model's front-layer parameters were fixed while later-layer parameters were fine-tuned. The target dataset was composed of time-frequency spectrum images of EEG signals. The experimental results showed a classification accuracy of 74.2%. A parallel multiscale filter bank CNN was proposed in [125]. This network achieved a classification accuracy of 75.8%, 84.3%, and 94.4% for three different public datasets. An alternative to discriminative FBCSP was proposed in [126] for a multiclass motor imagery signal. A frequency band was chosen for each binary combination of classes, and it was then entered into a matrix that feeds one or more CNNs that have already undergone Bayesian optimization. The proposed technique successfully achieved 81.6% classification accuracy.

Authors in [127] demonstrated novel MCNN and CCNN fusion methods. On public datasets, several experiments were conducted to evaluate the performance of CNN fusion approaches. Classification accuracy of 75.7% and 95.4% were attained using the suggested strategy. Li et al. [128] presented a densely feature fusion CNN (DFFN) that takes into account the correlation between neighboring layers and cross-layer features. It considered the network's local and

global properties and minimized information loss during convolutional operation. The proposed methodology achieved a classification accuracy of 79.7%. In [129], for learning subject-specific features, ConvNets used a combined space-time-frequency feature extraction method. When compared to traditional convolutional kernels, the Morlet wavelet used less parameters and gave the features learnt at the corresponding layer spectral amplitude. To establish the network for a new subject, subject-to-subject weight transfer was employed as parameters for the current subjects. They attained a classification accuracy of 74%. A data augmentation method and a hybrid-scale CNN architecture was proposed in [130]. On two widely used datasets, the suggested technique obtained average classification accuracy of 91.57% and 87.6%. In [131], an algorithm with a combination of transfer learning and CWT was proposed. On the binary class BCI dataset, the suggested approach had a 95.71% accuracy rate.

One-dimensional multi-scale CNN (1DMSCNN) and conditional EMD (CEMD) were presented in [132] to identify MI EEG data. The correlation coefficient between the initial EEG signal and each IMF was utilized as the first criterion in the CEMD algorithm to choose IMFs, and the second requirement was the relative energy occupancy rates between the IMFs. The CEMD algorithm acted as a denoising technique for EEG signals. Authors in [133] proposed a CNN using transfer learning and an end-to-end serial-parallel (SP) structure. The parallel domain was utilized for learning fine characteristics on various scales, whereas the serial domain was used to extract rough features from the time-frequency-space domain. Improved cross-subject entropy was achieved with the use of a freeze-and-retrain fine-tuning transfer learning technique. The suggested model reported an average testing accuracy of 72.13% and an average loss of 0.47. A pre-trained CNN with different optimizers, activation functions, and learning rates to process the MI dataset was considered in [134]. They achieved an accuracy of 99.52% on a binary class dataset with a pre-trained model of Shuffle-net with a learning rate of 0.0001. Authors in [135] used the algorithm of dimensionality reduction using perceptual loss. They proposed a subject transfer neural network (STNN), where a generator was used to generate useful attributes, then CNN based classifier provides an accuracy of 88.2% was achieved. PSO optimizer along with a light GBM classifier was studied in [136] to achieve a classification accuracy of 85.5% for the multiclass dataset. A parallel CNN architecture was proposed in [137] by creating a new image using spatial features and frequency bands of the MI signal simultaneously. The proposed strategy produced a kappa value of 0.65 and a classification accuracy of 83%. Khademi et al. [138] analyzed a CNN along with an LSTM classifier. They converted 1-D data into images and achieved a classification accuracy of 86%.

Table 8 provides a performance comparison of various deep-learning schemes, where the accuracy values are taken directly from the published works of the respective authors. Fig. 22 shows the different deep learning-based architectures employed by researchers for analysis of MI signals. it conclude that about two-thirds of the research works use CNNs whereas the rest use RNN, GAN, and some other hybrid architectures. Table 9 provides us the comparison of deep learning based techniques used in literature.

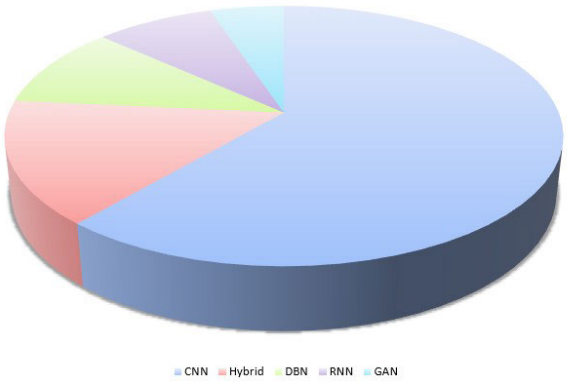

FIGURE 22. Deep learning-based architectures used for MI EEG data in literature.

VI. RESEARCH GAPS AND RECENT TRENDS

There has been an extensive research in the domain of BCI. However, there exist some active challenges which are due to the system-level limitations, such as the accuracy, reliability, and safety of the BCI devices and algorithms. Other challenges are related to the human-level limitations, such as the variability, adaptability, and ethics of the BCI users and their interactions with the technology. Data set is a challenging issue while dealing with the BCI system. Training the subject is one of the tedious task either in directing the subject or during the recording session. The mood of the same subject may differ at times which may lead to a change in signal. Different subjects act differently in several situations which may affect data. The subject must control his brain feedback signals during the recording of the session. Therefore, preparing a dataset remains a key challenge, and a time-consuming task. Further, it is exceedingly difficult to deal with data since it is nonlinear, non-stationary, and noisy at the same time. The brain being a complex nonlinear system, the brain waves/signals are also quite complex. Mental state, emotional state, fatigue level, and concentration level make the signal non-stationary, since they keep on changing at different time instants. The noise also becomes a significant challenge to deal with. It can occur due to the movement of electrodes, eye blinking, and some environmental disturbances. The small training set is a deterrent to attaining superior results. Deep learning techniques are data-hungry, so they require adequate training data to properly train the model. There occurs a trade-off between the technological complexity and the amount of training data.

Artifacts are also associated with EEG signals which need to be removed. As Section II explains, there are several kinds of artifacts. Since the causes of the various artifacts are different, the artifact-removal methods also need to be devised individually. As a result, there is a requirement for a

TABLE 8. Comparison of deep learning techniques.

Sr. No.	Author [Year]	Arch./Act. fun.	Input formulation	Dataset	Accuracy (%)
1	Tabar et al.[2016]	CNN/ReLU	STFT	BCI II 3	74.8
2	Schrimeister et al. [2017]	CNN/ELU	Time Series	BCI IV 2a BCI IV 2b	82.1 84
3	Sakhvi et al. [2018]	CNN/ReLU	FBCSP	BCI IV 2a	74.46
4	Han et al [2022]	CNN	STFT	BCI IV 2b	83
5	Hassanpour et al. [2019]	SAE	Time Series	BCI IV 2a	71
6	Wang et al. [2018]	LSTM/ Sigmoid	1-d	BCI IV 2a	71
7	Luo et al. [2018]	RNN/LSTM	FBCSP	BCI IV 2a BCI IV 2b	78.24 82.39
8	Lawhern et al. [2018]	CNN/ELU	Time Series	BCI IV 2a	67
9	Majidov et al. [2019]	CNN/ReLU	FBCSP	BCI IV 2a BCI IV 2b	80.44 82.39
10	Chaudhary et al. [2019]	CNN/ReLU	CWT	BCIC III 4a	99.35
11	Li et al. [2019]	CNN/ELU	Time Series	BCI IV 2a	74.6
12	Tayeb et al. [2019]	CNN/ReLU	Time Series	BCI IV 2b	84.24
13	Zhao et al. [2019]	CNN/ELU	3-D image	BCI IV 2a	52.17
14	Xu et al. [2019]	CNN/ReLU	STFT	BCI IV 2b	74.2
15	Wu et al. [2019]	CNN/Linear	Time Series	BCI IV 2b	84.3
16	Khedemi et al. [2022]	CNN/LSTM	CWT	BCI IV 2a	86
17	Amin et al. [2019]	CNN/ELU	Time Series	BCI IV 2a	75.7
18	Li et al. [2019]	CNN/ReLU	CSP		79.7
19	Zhao et al. [2019]	CNN/Linear	Time Series	BCI IV 2a	83
20	Dai et al. [2020]	CNN/ELU	Time Series	BCI IV 2a BCI IV 2b	91.5 87, 6
21	Sadiq et al. [2022]	CNN			99.52
22	Echeverri et al. [2019]	CNN/ReLU	BSS CWT	BCI III 4a	94.66
23	Tang et al. [2020]	CNN/ReLU	EMD	BCI IV 2b	82.61
24	Padila et al. [2019]	CNN/ReLU	FBCSP	BCI IV 2a	80.03
25	Kant et al. [2020]	CNN/ReLU	CWT	BCI II 3	95.71
26	Sun et al. [2022]	CNN	Time Series	BCI IV 2b	88.2
27	Abenna et al. [2022]	GBM	Time Series	BCI IV 2b	85.5
28	AK et al. [2021]	CNN	Time Series	Private Dataset	90
29	Zhao et al. [2021]	SPCNN	Time Series	BCI IV 2b	72.13

TABLE 9. Comparison of conventional and deep learning based approaches.

Conventional Signal Processing Techniques	Deep Learning Techniques
Based on mathematical transformations or decompositions	Based on artificial neural networks
Large amount of data increases the complexity	Require large amounts of data
Require prior knowledge or assumptions about the signal	Does not require prior knowledge or assumptions about the signal
Parameters like decomposition level, sampling frequency need to be set	Few parameters like batch size, epochs, learn rate, optimizer need to be set
Provide interpretable or explainable results	Provide black-box or opaque results
Well suited for linear or stationary signals	Suitable for nonlinear or non-stationary signals
Perform low-level or mid-level tasks	Perform high-level or end-to-end tasks

technique that can appropriately denoise a signal. Due to the presence of artifacts, feature extraction and selection become a challenging task while considering BCI systems. Feature extraction is performed in various domains as discussed in Section II-A3. These features perform well for binary class datasets but the performance drops for multiclass datasets. Therefore, an optimal technique is required for multiclass datasets as well. After feature extraction, the selection of suitable features is a big challenge. A specific set of features' performance varies for different subjects in the same dataset. Hence, a robust technique is required that works well across the entire dataset. After solving these problems, low information transfer rate (ITR), low signal-to-noise (SNR) ratio and robust algorithm also need to be resolved. Optimal evaluation metrics can be categorized into two parts information-based and classification-based. Information-based measures depend upon the probabilistic dependency and inter-class distance. Though the information-based metrics use one-time calculations, they do not promise the best results. Classification-based metrics depend on the error rate of the classifier. Classification performance results may be quite different as we change the classifier. Therefore, an appropriate classifier model needs to be developed for the said purpose. The impact of non-task-related activities is also a major concern for the performance of BCI systems [139]. Non task related brain activity is the brain activity that occurs when a person is not engaged in a specific cognitive or behavioral task, such as resting state activity or spontaneous fluctuations. Non task related brain activity may reveal the intrinsic functional architecture of the brain, as well as the variability in behavior and the physiological correlates of neurological and psychiatric disorders [14]. As alpha rhythm is more related to the motor-related cortex, a significant reduction in the amplitude of this wave is seen in the idle state [140]. Moreover, the response of different subjects for

the same MI task is different. As a specified set of subjects cannot be used every time for a successful experiment, it is referred to as ''BCI inefficiency'' [141]. In this, prediction of the user is also a pivotal point. Researchers have also performed experimentation on various physiological and neuro-physiological factors. Physiological factors such as being comfortable [142], attention span [143], fatigue [144], and neuro-physiological factors such as power of theta and alpha band [145], power of gamma oscillations [146], effect of resting state [147], shows their dependency on BCI performance.

Real-time performance is also a challenge for BCI systems. As the models are usually trained on data sets that are prepared in a controlled lab environment, they do not represent the intricacies of real-world scenarios, where every subject behaves differently with different environment. Therefore, a multi-task hybrid archetypal is needed that should be able to handle two tasks at the same time, one of which is individual identification and the other is class recognition. Availability of standard hardware is also a concern while recording data sets. As the head circumference for all the people cannot be the same for recording signals through all the channels, therefore, different numbers of head caps are needed. It is costly to arrange such a variety of head caps. Therefore, a robust and efficient system is required with stable performance that can be used by different users in different environments having different mental states. Currently BCI is widely used only in medical field, but it needs to be explored in other areas as well, for example, it can have more applications in home automation and entertainment. Various application fields can be seen as disease detection, refunctioning of central nervous system, neuroergonomics, games, and entertainment, for smart homes. BCI for smart homes is an intriguing area of study that can let the user control electrical devices, lights, and provide workable home automation [148]. Authors in [149] developed a software application named back home which provides an ultimate standard of living with its overwhelming features.

Disease detection and diagnosis at an early stage can help a patient avoid any damage to the organ. Abnormal brain structure (brain tumor), epilepsy, sleep apnea, and brain swelling (such as encephalitis) are different abnormalities associated with the brain that are currently diagnosed with the help of MRI and CT-scan. The sleep apnea disease is narcolepsy that can be detected with the help of EEG recording [150]. Sleep apnea has three main categories: central sleep apnea (CSA), obstructive sleep apnea (OSA), and mixed sleep apnea (MSA). OSA is a quite ordinary sleep disorder characterized by morning headaches and loud snoring. Due to this, upper airway is completely blocked and throat muscles are relaxed to block airways. CSA is a harmful disorder in which signals that are controlling breadth are stopped by the brain. It may cause heart failure and stroke. MSA is a combination of the above-explained disorders. It is also the main diagnostic for epilepsy. We can detect a seizure and a non-seizure signal for confirmation of epilepsy. Brain tumors, brain damage due to any head injury, encephalitis, encephalopathy (brain dysfunction), and brain dead are detected with the help of EEG signals.

Responsiveness is a pivotal factor while discussing about the real-time performance of the BCI system. Responsiveness is the response time against a decision factor i.e. the time from the moment of stimulus to the decision made(correct/incorrect) [151]. This is a vital component in the effective implementation of BCIs for various applications such as communication, control, and rehabilitation. the type of brain signal, quality of the signal, and complexity of the task are considerable factors for evaluating the performance of BCI systems. Signal detection, signal translation, and fatigue are a few common challenges for enhancing the responsiveness of the BCI system [152]. Though there are some tools for evaluating BCI response such as the evaluation interface, PROEZA SG with BCI that includes the parameter of response time, type of decision, and decision holding time. Researchers used deep learning-based techniques and used multiple EEG channels to get a better electrical signal of the brain and improve the responsiveness of the system [153], [154].

BCI devices for communication are a new communication and control channel that helps us to restore the function of motor nerves in the external world [155]. The brain can be monitored by EEG, functional magnetic resonance imaging (fMRI), positron emission tomography (PET), magnetoencephalography (MEG), and optical imaging. However, the time constant for each of these methods is rather large as they depend upon blood flow. Therefore, they cannot communicate fast. However, EEG has a fleeting time constant and can be used for faster communication. Biometric identification for security and validation can also be an application under BCI [156]. It is related to individual identification like fingerprint, retinal data, face recognition, and voice. EEG-based biometry has some issues regarding robustness, security, privacy, and ergonomics, and research is needed for efficient simulation which can be adapted for subject identification in BCI systems and applications.

Therapy and assessment give us a quick, cheap, portable, and user-friendly way to recognize emotions [157]. Emotional states are controlled by the frontal and parietal lobes of the brain, while a few brain-like beta waves appear to be the most discriminative. The common belief that women are more emotional than men is found consistent with EEG as well. EEGs do multichannel recordings from both the central and the autonomous nervous systems. In affective neuroscience, feelings can be viewed as a subjective illustration of emotions. Moods are affected by emotions which have an impact for an exceedingly long duration than emotions and are also commonly less affected than emotions. Neuroergonomics is a study that deals with support enhancement in the workplace [158]. With this, we can understand the fatigue level of a worker, and his interests at the time of work. We can convert our place into a smart workplace where different activities could be done in an efficient manner.

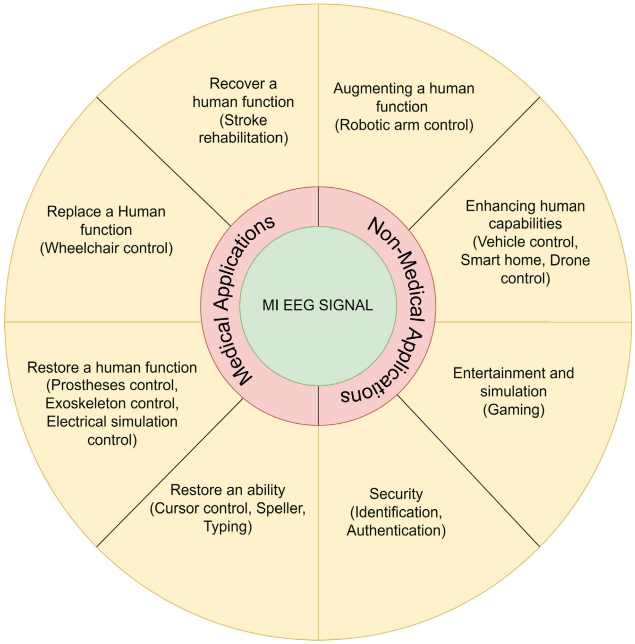

FIGURE 23. Various applications of MI EEG.

BCI for entertainment has emerged as a noteworthy discovery for gamers. Mind control game is a forthcoming facility that will be provided to the entertainment field [55]. BCI-based games recognize the interest of the gamer, extent of involvement in the game, and the level of stress during the game. It also controls the difficulty level in multiplayer games. EEG data is used to monitor the excitement of the player and dynamic difficulty adjustment can be performed according to the interest of the player. Fig. 23 shows various applications fields associated with MI EEG datasets. these can be divided in two categorizations as medical and non-medical. Medical applications include restoring, replacing, and regenerating human abilities and functions whereas non-medical applications relate to home automation, entertainment, and security.

In future, researchers may convert EEG data into 2-D data. It is quite easy and approachable to use images as compared to 1-D data, especially for deep-learning schemes. Different pre-trained networks are available to train on these image datasets. Since they have already learnt some weights, it becomes convenient to use these networks. These pre-trained networks converge on small datasets as well. Some well-known pre-trained networks are Google-net, AlexNet, VGG-19, inception, etc. Attention mechanism and reinforcement learning are also in trend which may be a solution for robust and general framework. Attention approach focuses on the most dominant features of the signal which result in better performance whereas reinforcement learning has the ability to identify important components of signals [159]. A zero calibration BCI system is needed for subject independent classification which can be solved by customizing a model using transfer learning approach. Further, Deep learning algorithms used for decision-making can perform better with additional data augmentation techniques. Fusion techniques may also be used for improving the results, where both the conventional and deep learning-based techniques are combined to obtain the results. In fusion techniques, we can use the advantages of both methods. Fusion is possible at three different levels: input, feature, and decision.

VII. CONCLUSION

There are several challenges in analyzing BCI EEG signals, therefore, we require a systematic and robust approach to deal with these challenges. The performance of signal processing-based techniques for BCI MI analysis depends on signal processing steps, denoising, and efficient feature extraction and selection. various pre-processing steps, followed by sampling and filtering. Various time-domain, frequency-domain, time-frequency domain, and nonlinear signal processing techniques have been discussed in this article. In addition to this, feature selection and transformation methods are also included under signal processing techniques. The performance of deep-learning approaches majorly rely on the size of dataset, depth of architecture and transfer learning approach. Various deep-learning approaches for analyzing EEG data have been discussed in detail. Widely-used classifiers have also been reviewed. Further, publicly available BCI MI-EEG datasets are presented, which may be used for future research activities in this domain. Conventional signal processing techniques provide mathematical formulations which give good accuracy on smaller datasets, however, they their performance drops as the dataset gets larger. But with larger datasets, deep learning algorithms performs better as these are data-hungry algorithms. Future work related to BCI MI should investigate techniques which are less computationally complex, yield superior performance measures, and can generalize on a smaller dataset. The technique should be robust enough to handle high-dimensionality data with noisy signals.

ACKNOWLEDGMENT

The authors would like to acknowledge the support from Intelligent Prognostic Private Limited Delhi, India researcher's supporting Project for funding this research work. The authors would like to acknowledge the support from Universiti Sultan Zainal Abidin - UniSZA (UniSZA) Malaysia.

REFERENCES

[1] A. Kawala-Sterniuk, M. Pelc, R. Martinek, and G. M. Wójcik, "Editorial: Currents in biomedical signals processing—Methods and applications," *Frontiers Neurosci.*, vol. 16, Jul. 2022, Art. no. 989400.
[2] H. M. Rai and K. Chatterjee, "Hybrid CNN-LSTM deep learning model and ensemble technique for automatic detection of myocardial infarction using big ECG data," *Int. J. Speech Technol.*, vol. 52, no. 5, pp. 5366–5384, Mar. 2022.
[3] M. R. Kose, M. K. Ahirwal, and A. Kumar, "A new approach for emotions recognition through EOG and EMG signals," *Signal, Image Video Process.*, vol. 15, no. 8, pp. 1863–1871, May 2021.
[4] E. B. N. Friedel, L. Tebartz van Elst, C. Schmelz, D. Ebert, S. Maier, D. Endres, K. Runge, K. Domschke, E. Bubl, J. Kornmeier, M. Bach, S. P. Heinrich, and K. Nickel, "Replication of reduced pattern electroretinogram amplitudes in depression with improved recording parameters," *Frontiers Med.*, vol. 8, pp. 1–10, Oct. 2021.

[5] D. D. Yigit, M. O. Sevik, and Ö. Şahin, "Transcorneal electrical stimulation therapy may have a stabilization effect on multifocal electroretinography for patients with retinitis pigmentosa," *Retina*, vol. 42, no. 5, pp. 923–933, May 2022.

[6] S. S. Poorna, R. Raghav, A. Nandan, and G. J. Nair, "EEG based control—A study using wavelet features," in *Proc. Int. Conf. Adv. Comput., Commun. Informat. (ICACCI)*, Sep. 2018, pp. 550–553.

[7] A. Soler, L. A. Moctezuma, E. Giraldo, and M. Molinas, "Automated methodology for optimal selection of minimum electrode subsets for accurate EEG source estimation based on genetic algorithm optimization," *Sci. Rep.*, vol. 12, no. 1, pp. 1–18, Jul. 2022.

[8] I. A. Kershner, M. V. Sinkin, and Y. V. Obukhov, "Detection of epileptic seizures in EEG signals during long-term monitoring of patients after traumatic brain injury," *J. Phys., Conf. Ser.*, vol. 1368, no. 5, Nov. 2019, Art. no. 052007.

[9] J. N. Acharya, A. Hani, J. Cheek, P. Thirumala, and T. N. Tsuchida, "American clinical neurophysiology society guideline 2: Guidelines for standard electrode position nomenclature," *J. Clin. Neurophysiol., Off. Publication Amer. Electroencephalographic Soc.*, vol. 33, no. 4, pp. 308–311, 2016.

[10] K. B. E. Böcker, J. A. G. van Avermaete, and M. M. C. van den Berg-Lenssen, "The international 10–20 system revisited: Cartesian and spherical co-ordinates," *Brain Topography*, vol. 6, no. 3, pp. 231–235, Mar. 1994.

[11] M. K. Delimayanti, B. Purnama, N. G. Nguyen, M. R. Faisal, K. R. Mahmudah, F. Indriani, M. Kubo, and K. Satou, "Classification of brainwaves for sleep stages by high-dimensional FFT features from EEG signals," *Appl. Sci.*, vol. 10, no. 5, p. 1797, Mar. 2020.

[12] J. S. Kumar and P. Bhuvaneswari, "Analysis of electroencephalography (EEG) signals and its categorization—A study," *Proc. Eng.*, vol. 38, pp. 2525–2536, Jan. 2012.

[13] Y. S. Singh, "A review paper on brain-computer interface," *Int. J. Eng. Res. Technol.*, vol. 3, no. 10, pp. 1–6, doi: 10.17577/IJERTCONV3IS10102.

[14] M. F. Mridha, S. C. Das, M. M. Kabir, A. A. Lima, M. R. Islam, and Y. Watanobe, "Brain-computer interface: Advancement and challenges," *Sensors*, vol. 21, no. 17, p. 5746, Aug. 2021.

[15] A. Miladinović, A. Barbaro, E. Valvason, M. Ajčević, A. Accardo, P. P. Battaglini, and J. Jarmolowska, "Combined and singular effects of action observation and motor imagery paradigms on resting-state sensorimotor rhythms," in *Proc. Mediterranean Conf. Med. Biol. Eng. Comput.* Coimbra, Portugal: Springer, 2020, pp. 1129–1137.

[16] N. Kosmyna and A. Lécuyer, "A conceptual space for EEG-based brain-computer interfaces," *PLoS ONE*, vol. 14, no. 1, Jan. 2019, Art. no. e0210145.

[17] S. N. Abdulkader, A. Atia, and M.-S.-M. Mostafa, "Brain computer interfacing: Applications and challenges," *Egyptian Informat. J.*, vol. 16, no. 2, pp. 213–230, Jul. 2015.

[18] D. Gorjan, K. Gramann, K. De Pauw, and U. Marusic, "Removal of movement-induced EEG artifacts: Current state of the art and guidelines," *J. Neural Eng.*, 2022.

[19] G. Madhale Jadav, J. Lerga, and I. Štajduhar, "Adaptive filtering and analysis of EEG signals in the time-frequency domain based on the local entropy," *EURASIP J. Adv. Signal Process.*, vol. 2020, no. 1, pp. 1–18, Dec. 2020.

[20] X. Jiang, G. B. Bian, and Z. Tian, "Removal of artifacts from EEG signals: A review," *Sensors*, vol. 19, no. 5, p. 987, 2019, doi: 10.3390/s19050987.

[21] O. Aydemir, S. Pourzare, and T. Kayikcioglu, "Classifying various EMG and EOG artifacts in EEG signals," *Przeglad Elektrotechniczny*, vol. 88, no. 11A, pp. 218–222, 2012.

[22] M. K. Islam, P. Ghorbanzadeh, and A. Rastegarnia, "Probability mapping based artifact detection and removal from single-channel EEG signals for brain–computer interface applications," *J. Neurosci. Methods*, vol. 360, Aug. 2021, Art. no. 109249.

[23] A. S. Al-Fahoum and A. A. Al-Fraihat, "Methods of EEG signal features extraction using linear analysis in frequency and time-frequency domains," *ISRN Neurosci.*, vol. 2014, pp. 1–7, Feb. 2014.

[24] P. Singh, S. D. Joshi, R. Kumar, and K. Saha, "The Fourier decomposition method for nonlinear and non-stationary time series analysis Subject Areas," *Proc. Roy. Soc. A, Math., Phys. Eng. Sci.*, vol. 473, no. 2199, 2017.

[25] A. Prakash, "Wavelet and its applications," *Int. J. Sci. Res. Comput. Sci., Eng. Inf. Technol.*, vol. 3, pp. 95–104, Nov. 2018.

[26] A. Katharotiya, S. Patel, and M. Goyani, "Comparative analysis between DCT & DWT techniques of image compression," *J. Inf. Eng. Appl.*, vol. 1, no. 2, pp. 9–17, 2011.

[27] B. Fatimah, P. Singh, A. Singhal, and R. B. Pachori, "Detection of apnea events from ECG segments using Fourier decomposition method," *Biomed. Signal Process. Control*, vol. 61, Aug. 2020, Art. no. 102005.

[28] P. M. Tripathi, A. Kumar, R. Komaragiri, and M. Kumar, "Watermarking of ECG signals compressed using Fourier decomposition method," *Multimedia Tools Appl.*, vol. 81, no. 14, pp. 19543–19557, Jan. 2022.

[29] S. Mamli and H. Kalbkhani, "Gray-level co-occurrence matrix of Fourier synchro-squeezed transform for epileptic seizure detection," *Biocybern. Biomed. Eng.*, vol. 39, no. 1, pp. 87–99, Jan. 2019.

[30] M. K. I. Molla, S. Das, M. E. Hamid, and K. Hirose, "Empirical mode decomposition for advanced speech signal processing," *J. Signal Process.*, vol. 17, no. 6, pp. 215–229, 2013.

[31] U. Maji and S. Pal, "Empirical mode decomposition vs. Variational mode decomposition on ECG signal processing: A comparative study," in *Proc. Int. Conf. Adv. Comput., Commun. Informat. (ICACCI)*, Sep. 2016, pp. 1129–1134.

[32] M. E. Abdulmunem and A. A. Badr, "Hilbert transform and its applications: A survey," *Int. J. Sci. Eng. Res.*, vol. 8, pp. 699–704, Feb. 2017.

[33] N. Bajaj, J. R. Carrión, F. Bellotti, R. Berta, and A. D. Gloria, "Automatic and tunable algorithm for EEG artifact removal using wavelet decomposition with applications in predictive modeling during auditory tasks," *Biomed. Signal Process. Control*, vol. 55, Jan. 2020, Art. no. 101624.

[34] P. M. Tripathi, A. Kumar, R. Komaragiri, and M. Kumar, "A novel approach for real-time ECG signal denoising using Fourier decomposition method," *Res. Biomed. Eng.*, vol. 38, pp. 1037–1049, Sep. 2022.

[35] Q. Cheng, W. Yang, K. Liu, W. Zhao, L. Wu, L. Lei, T. Dong, N. Hou, F. Yang, Y. Qu, and Y. Yang, "Increased sample entropy in EEGs during the functional rehabilitation of an injured brain," *Entropy*, vol. 21, no. 7, p. 698, Jul. 2019.

[36] P. Memar and F. Faradji, "A novel multi-class EEG-based sleep stage classification system," *IEEE Trans. Neural Syst. Rehabil. Eng.*, vol. 26, no. 1, pp. 84–95, Jan. 2018.

[37] M. Saini, U. Satija, and M. D. Upadhayay, "One-dimensional convolutional neural network architecture for classification of mental tasks from electroencephalogram," *Biomed. Signal Process. Control*, vol. 74, Apr. 2022, Art. no. 103494.

[38] R. Ul Alam, H. Zhao, A. Goodwin, O. Kavehei, and A. McEwan, "Differences in power spectral densities and phase quantities due to processing of EEG signals," *Sensors*, vol. 20, no. 21, pp. 1–20, 2020.

[39] P. Jain and R. B. Pachori, "An iterative approach for decomposition of multi-component non-stationary signals based on eigenvalue decomposition of the Hankel matrix," *J. Franklin Inst.*, vol. 352, no. 10, pp. 4017–4044, Oct. 2015.

[40] F. Anowar, S. Sadaoui, and B. Selim, "Conceptual and empirical comparison of dimensionality reduction algorithms (PCA, KPCA, LDA, MDS, SVD, LLE, ISOMAP, LE, ICA, t-SNE)," *Comput. Sci. Rev.*, vol. 40, May 2021, Art. no. 100378.

[41] J. V. Stone, "Independent component analysis," in *Neural Information Theory*, P. E. Latham and A. Pouget, Eds. MIT Press, Feb. 2005, pp. 155–178.

[42] A. Miladinović, M. Ajčević, and A. Accardo, "Performance of dual-augmented Lagrangian method and common spatial patterns applied in classification of motor-imagery BCI," 2020, *arXiv:2010.10359*.

[43] A. Miladinović, M. Ajčević, J. Jarmolowska, U. Marusic, M. Colussi, G. Silveri, P. P. Battaglini, and A. Accardo, "Effect of power feature covariance shift on BCI spatial-filtering techniques: A comparative study," *Comput. Methods Programs Biomed.*, vol. 198, Jan. 2021, Art. no. 105808.

[44] H. He and D. Wu, "Spatial filtering for brain computer interfaces: A comparison between the common spatial pattern and its variant," in *Proc. IEEE Int. Conf. Signal Process., Commun. Comput. (ICSPCC)*, Sep. 2018, pp. 1–6.

[45] A. S. Aghaei, M. S. Mahanta, and K. N. Plataniotis, "Separable common spatio-spectral patterns for motor imagery BCI systems," *IEEE Trans. Biomed. Eng.*, vol. 63, no. 1, pp. 15–29, Jan. 2016.

[46] Y. Zhang, C. S. Nam, G. Zhou, J. Jin, X. Wang, and A. Cichocki, "Temporally constrained sparse group spatial patterns for motor imagery BCI," *IEEE Trans. Cybern.*, vol. 49, no. 9, pp. 3322–3332, Sep. 2019.

[47] T. Long, M. Wan, W. Jian, H. Dai, W. Nie, and J. Xu, "Application of multi-task transfer learning: The combination of EA and optimized subband regularized CSP to classification of 8-channel EEG signals with small dataset," *Frontiers Hum. Neurosci.*, vol. 17, Mar. 2023, Art. no. 1143027.
[48] D. Garrett, D. A. Peterson, C. W. Anderson, and M. H. Thaut, "Comparison of linear, nonlinear, and feature selection methods for EEG signal classification," *IEEE Trans. Neural Syst. Rehabil. Eng.*, vol. 11, no. 2, pp. 141–144, Jun. 2003.
[49] M. R. N. Kousarrizi, A. A. Ghanbari, M. Teshnehlab, M. A. Shorehdeli, and A. Gharaviri, "Feature extraction and classification of EEG signals using wavelet transform, SVM and artificial neural networks for brain computer interfaces," in *Proc. Int. Joint Conf. Bioinf., Syst. Biol. Intell. Comput.*, Aug. 2009, pp. 352–355.
[50] A. Bablani, D. R. Edla, and S. Dodia, "Classification of EEG data using k-nearest neighbor approach for concealed information test," *Proc. Comput. Sci.*, vol. 143, pp. 242–249, Jan. 2018.
[51] Y. Roy, H. Banville, I. Albuquerque, A. Gramfort, T. H. Falk, and J. Faubert, "Deep learning-based electroencephalography analysis: A systematic review," *J. Neural Eng.*, vol. 16, no. 5, Aug. 2019, Art. no. 051001.
[52] A. Afthanorhan, A. Mahmud, A. Sapri, N. Aimran, A. Aireen, and A. Rambli, "Prediction of Malaysian women divorce using machine learning techniques," *MALAYSIAN J. OF Comput.*, vol. 7, no. 2, pp. 1149–1161, 2022.
[53] N. S. Bastos, B. P. Marques, D. F. Adamatti, and Cleo Z. Billa, "Analyzing EEG signals using decision trees: A study of modulation of amplitude," *Comput. Intell. and Neurosci.*, vol. 2020, Jul. 2020, Art. no. 32695151.
[54] R. Sharma, M. Kim, and A. Gupta, "Motor imagery classification in brain-machine interface with machine learning algorithms: Classical approach to multi-layer perceptron model," *Biomed. Signal Process. Control*, vol. 71, Jan. 2022, Art. no. 103101.
[55] A. Al-Saegh, S. A. Dawwd, and J. M. Abdul-Jabbar, "Deep learning for motor imagery EEG-based classification: A review," *Biomed. Signal Process. Control*, vol. 63, Jan. 2021, Art. no. 102172.
[56] A. M. Roy, "An efficient multi-scale CNN model with intrinsic feature integration for motor imagery EEG subject classification in brain-machine interfaces," *Biomed. Signal Process. Control*, vol. 74, Apr. 2022, Art. no. 103496.
[57] W. Ma, H. Xue, X. Sun, S. Mao, L. Wang, Y. Liu, Y. Wang, and X. Lin, "A novel multi-branch hybrid neural network for motor imagery EEG signal classification," *Biomed. Signal Process. Control*, vol. 77, Aug. 2022, Art. no. 103718.
[58] S. Kwon, "A CNN-assisted enhanced audio signal processing for speech emotion recognition," *Sensors*, vol. 20, no. 1, p. 183, Dec. 2019.
[59] W. Wei, W. Yang, E. Zuo, Y. Qian, and L. Wang, "Person re-identification based on deep learning—An overview," *J. Vis. Commun. Image Represent.*, vol. 82, Jan. 2022, Art. no. 103418.
[60] M. Riyad, M. Khalil, and A. Adib, "MI-EEGNET: A novel convolutional neural network for motor imagery classification," *J. Neurosci. Methods*, vol. 353, Apr. 2021, Art. no. 109037.
[61] B. Xu, L. Zhang, A. Song, C. Wu, W. Li, D. Zhang, G. Xu, H. Li, and H. Zeng, "Wavelet transform time-frequency image and convolutional network-based motor imagery EEG classification," *IEEE Access*, vol. 7, pp. 6084–6093, 2019.
[62] Y. Khalifa, D. Mandic, and E. Sejdić, "A review of hidden Markov models and recurrent neural networks for event detection and localization in biomedical signals," *Inf. Fusion*, vol. 69, pp. 52–72, May 2021.
[63] A. Craik, Y. He, and J. L. Contreras-Vidal, "Deep learning for electroencephalogram (EEG) classification tasks: A review," *J. Neural Eng.*, vol. 16, no. 3, Apr. 2019, Art. no. 031001.
[64] S. Kumar, A. Sharma, and T. Tsunoda, "Brain wave classification using long short-term memory network based OPTICAL predictor," *Sci. Rep.*, vol. 9, no. 1, p. 9153, Jun. 2019.
[65] S. Gao, Y. Huang, S. Zhang, J. Han, G. Wang, M. Zhang, and Q. Lin, "Short-term runoff prediction with GRU and LSTM networks without requiring time step optimization during sample generation," *J. Hydrol.*, vol. 589, Oct. 2020, Art. no. 125188.
[66] Y. Wang, M. Zhang, R. Wu, H. Wang, Z. Luo, and G. Li, "Speech neuromuscular decoding based on spectrogram images using conformal predictors with bi-LSTM," *Neurocomputing*, vol. 451, pp. 25–34, Sep. 2021.
[67] J. Liu, L. Zhang, H. Wu, and H. Zhao, "Transformers for EEG emotion recognition," 2021, *arXiv:2110.06553*.
[68] N. Lu, T. Li, X. Ren, and H. Miao, "A deep learning scheme for motor imagery classification based on restricted Boltzmann machines," *IEEE Trans. Neural Syst. Rehabil. Eng.*, vol. 25, no. 6, pp. 566–576, Jun. 2017.
[69] M. Z. Alom, T. M. Taha, C. Yakopcic, S. Westberg, P. Sidike, M. S. Nasrin, M. Hasan, B. C. Van Essen, A. A. Awwal, and V. K. Asari, "A state-of-the-art survey on deep learning theory and architectures," *Electronics*, vol. 8, no. 3, pp. 1–67, 2019.
[70] E. Hernández-González, P. Gómez-Gil, E. Bojorges-Valdez, and M. Ramírez-Cortés, "Bi-dimensional representation of EEGs for BCI classification using CNN architectures," in *Proc. 43rd Annu. Int. Conf. IEEE Eng. Med. Biol. Soc. (EMBC)*, Nov. 2021, pp. 767–770.
[71] K. Zhang, G. Xu, Z. Han, K. Ma, X. Zheng, L. Chen, N. Duan, and S. Zhang, "Data augmentation for motor imagery signal classification based on a hybrid neural network," *Sensors*, vol. 20, no. 16, pp. 1–20, 2020.
[72] J. Yang, H. Yu, T. Shen, Y. Song, and Z. Chen, "4-class MI-EEG signal generation and recognition with CVAE-GAN," *Appl. Sci.*, vol. 11, no. 4, p. 1798, Feb. 2021.
[73] C. Li, H. Yang, X. Wu, and Y. Zhang, "Improving EEG-based motor imagery classification using hybrid neural network," in *Proc. IEEE 9th Int. Conf. Inf., Commun. Netw. (ICICN)*, Nov. 2021, pp. 486–489.
[74] H. Li, M. Ding, R. Zhang, and C. Xiu, "Motor imagery EEG classification algorithm based on CNN-LSTM feature fusion network," *Biomed. Signal Process. Control*, vol. 72, Feb. 2022, Art. no. 103342.
[75] R. H. Elessawy, S. Eldawlatly, and H. M. Abbas, "A long short-term memory autoencoder approach for EEG motor imagery classification," in *Proc. Int. Conf. Comput., Autom. Knowl. Manage. (ICCAKM)*, Jan. 2020, pp. 79–84.
[76] J. Xie, C. Siyu, Y. Zhang, D. Gao, and T. Liu, "Combining generative adversarial network and multi-output CNN for motor imagery classification," *J. Neural Eng.*, vol. 18, no. 4, Mar. 2021, Art. no. 046026.
[77] A. L. Goldberger, L. A. N. Amaral, L. Glass, J. M. Hausdorff, P. C. Ivanov, R. G. Mark, J. E. Mietus, G. B. Moody, C.-K. Peng, and H. E. Stanley, "PhysioBank, PhysioToolkit, and PhysioNet: Components of a new research resource for complex physiologic signals," *Circulation*, vol. 101, no. 23, pp. E215–E220, Jun. 2000.
[78] F. Darvas, R. Scherer, J. G. Ojemann, R. P. Rao, K. J. Miller, and L. B. Sorensen, "High gamma mapping using EEG," *NeuroImage*, vol. 49, no. 1, pp. 930–938, Jan. 2010.
[79] M. Tangermann, K.-R. Müller, A. Aertsen, N. Birbaumer, C. Braun, C. Brunner, R. Leeb, C. Mehring, K. J. Miller, G. R. Müller-Putz, G. Nolte, G. Pfurtscheller, H. Preissl, G. Schalk, A. Schlögl, C. Vidaurre, S. Waldert, and B. Blankertz, "Review of the BCI competition IV," *Frontiers Neurosci.*, vol. 6, pp. 6–55, Jul. 2012.
[80] B. Blankertz, K.-R. Müller, D. J. Krusienski, G. Schalk, J. R. Wolpaw, A. Schlogl, G. Pfurtscheller, J. R. Millan, M. Schroder, and N. Birbaumer, "The BCI competition III: Validating alternative approaches to actual BCI problems," *IEEE Trans. Neural Syst. Rehabil. Eng.*, vol. 14, no. 2, pp. 153–159, Jun. 2006.
[81] P. Tripathi, A. Kumar, R. Komaragiri, and M. Kumar, "A review on computational methods for denoising and detecting ECG signals to detect cardiovascular diseases," *Arch. Comput. Methods Eng.*, vol. 29, no. 1, pp. 1–40, Oct. 2021.
[82] T. N. Alotaiby, S. A. Alshebeili, T. Alshawi, I. Ahmad, and F. E. A. El-Samie, "EEG seizure detection and prediction algorithms: A survey," *EURASIP J. Adv. Signal Process.*, vol. 2014, no. 1, p. 183, Dec. 2014.
[83] C. Arora, P. Khetarpal, S. Gupta, N. Fatema, H. Malik, and A. Afthanorhan, "Mathematical modelling to predict the effect of vaccination on delay and rise of COVID-19 cases management," *Mathematics*, vol. 11, no. 4, p. 821, Feb. 2023.
[84] T. Kuremoto, Y. Baba, M. Obayashi, S. Mabu, and K. Kobayashi, "Enhancing EEG signals recognition using ROC curve," *J. Robot., Netw. Artif. Life*, vol. 4, no. 4, p. 283, 2018.
[85] H. Malik, A. Afthanorhan, N. A. Amirah, and N. Fatema, "Machine learning approach for targeting and recommending a product for project management," *Mathematics*, vol. 9, no. 16, p. 1958, Aug. 2021.
[86] J. Kevric and A. Subasi, "Comparison of signal decomposition methods in classification of EEG signals for motor-imagery BCI system," *Biomed. Signal Process. Control*, vol. 31, pp. 398–406, Jan. 2017.

[87] V. Gupta, T. Priya, A. K. Yadav, R. B. Pachori, and U. Rajendra Acharya, "Automated detection of focal EEG signals using features extracted from flexible analytic wavelet transform," *Pattern Recognit. Lett.*, vol. 94, pp. 180–188, Jul. 2017.

[88] H. Göksu, "BCI oriented EEG analysis using log energy entropy of wavelet packets," *Biomed. Signal Process. Control*, vol. 44, pp. 101–109, Jul. 2018.

[89] S. Taran, V. Bajaj, D. Sharma, S. Siuly, and A. Sengur, "Features based on analytic IMF for classifying motor imagery EEG signals in BCI applications," *Measurement*, vol. 116, pp. 68–76, Feb. 2018.

[90] A. Bhattacharyya, L. Singh, and R. B. Pachori, "Fourier–Bessel series expansion based empirical wavelet transform for analysis of non-stationary signals," *Digit. Signal Process.*, vol. 78, pp. 185–196, Jul. 2018.

[91] J. Zhou, M. Meng, Y. Gao, Y. Ma, and Q. Zhang, "Classification of motor imagery EEG using wavelet envelope analysis and LSTM networks," in *Proc. Chin. Control Decis. Conf. (CCDC)*, Jun. 2018, pp. 5600–5605.

[92] A. Khalaf, E. Sejdic, and M. Akcakaya, "Common spatial pattern and wavelet decomposition for motor imagery EEG-fTCD brain-computer interface," *J. Neurosci. Methods*, vol. 320, pp. 98–106, May 2019.

[93] Ji, Ma, Dong, and Zhang, "EEG signals feature extraction based on DWT and EMD combined with approximate entropy," *Brain Sci.*, vol. 9, no. 8, p. 201, Aug. 2019.

[94] S. Ganorkar and V. Raut, "Comparative analysis of mother wavelet selection for EEG signal application to motor imagery based brain-computer interface," *Int. J. Sci. Technol. Res.*, vol. 8, no. 12, pp. 1001–1007, 2019.

[95] N. Bagh, R. Machireddy, and F. Shahlaei, "Classification of motor imagery tasks using phase space reconstruction and empirical mode decomposition," in *Proc. IEEE Can. Conf. Electr. Comput. Eng. (CCECE)*, May 2019, pp. 1–4.

[96] Q. Ai, A. Chen, K. Chen, Q. Liu, T. Zhou, S. Xin, and Z. Ji, "Feature extraction of four-class motor imagery EEG signals based on functional brain network," *J. Neural Eng.*, vol. 16, no. 2, Feb. 2019, Art. no. 026032.

[97] K. Venkatachalam, A. Devipriya, J. Maniraj, M. Sivaram, A. Ambikapathy, and I. S. Amiri, "A novel method of motor imagery classification using EEG signal," *Artif. Intell. Med.*, vol. 103, Mar. 2019, Art. no. 101787.

[98] L. Wang, X. Liu, Z. Liang, Z. Yang, and X. Hu, "Analysis and classification of hybrid BCI based on motor imagery and speech imagery," *Measurement*, vol. 147, Dec. 2019, Art. no. 106842.

[99] M. T. Sadiq, X. Yu, Z. Yuan, Z. Fan, A. U. Rehman, G. Li, and G. Xiao, "Motor imagery EEG signals classification based on mode amplitude and frequency components using empirical wavelet transform," *IEEE Access*, vol. 7, pp. 127678–127692, 2019.

[100] R. Zhang, Q. Zong, L. Dou, and X. Zhao, "A novel hybrid deep learning scheme for four-class motor imagery classification," *J. Neural Eng.*, vol. 16, no. 6, Oct. 2019, Art. no. 066004.

[101] S. Chaudhary, S. Taran, V. Bajaj, and S. Siuly, "A flexible analytic wavelet transform based approach for motor-imagery tasks classification in BCI applications," *Comput. Methods Programs Biomed.*, vol. 187, Apr. 2020, Art. no. 105325.

[102] E. M. dos Santos, R. Cassani, T. H. Falk, and F. J. Fraga, "Improved motor imagery brain-computer interface performance via adaptive modulation filtering and two-stage classification," *Biomed. Signal Process. Control*, vol. 57, Mar. 2020, Art. no. 101812.

[103] V. K. Mehla, A. Singhal, and P. Singh, "A novel approach for automated alcoholism detection using Fourier decomposition method," *J. Neurosci. Methods*, vol. 346, Dec. 2020, Art. no. 108945.

[104] F. Li, F. He, F. Wang, D. Zhang, Y. Xia, and X. Li, "A novel simplified convolutional neural network classification algorithm of motor imagery EEG signals based on deep learning," *Appl. Sci.*, vol. 10, no. 5, p. 1605, 2020.

[105] S. Taheri, M. Ezoji, and S. M. Sakhaei, "Convolutional neural network based features for motor imagery EEG signals classification in brain–computer interface system," *Social Netw. Appl. Sci.*, vol. 2, no. 4, p. 555, Apr. 2020.

[106] A. Echtioui, A. Mlaouah, W. Zouch, M. Ghorbel, C. Mhiri, and H. Hamam, "A novel convolutional neural network classification approach of motor-imagery EEG recording based on deep learning," *Appl. Sci.*, vol. 11, no. 21, p. 9948, Oct. 2021.

[107] G. Roy, A. K. Bhoi, and S. Bhaumik, "A comparative approach for MI-based EEG signals classification using energy, power and entropy," *IRBM*, vol. 43, no. 5, pp. 434–446, 2021.

[108] V. K. Mehla, A. Singhal, P. Singh, and R. B. Pachori, "An efficient method for identification of epileptic seizures from EEG signals using Fourier analysis," *Phys. Eng. Sci. Med.*, vol. 44, no. 2, pp. 443–456, Jun. 2021.

[109] T. Thenmozhi and R. Helen, "Feature selection using extreme gradient boosting Bayesian optimization to upgrade the classification performance of motor imagery signals for BCI," *J. Neurosci. Methods*, vol. 366, Jan. 2022, Art. no. 109425.

[110] X. Geng, S. Xue, P. Yu, D. Li, M. Yue, X. Zhang, and L. Wang, "A fusion algorithm for EEG signal processing based on motor imagery brain-computer interface," *Wireless Commun. Mobile Comput.*, vol. 2022, pp. 1–14, Mar. 2022.

[111] Y. R. Tabar and U. Halici, "A novel deep learning approach for classification of EEG motor imagery signals," *J. Neural Eng.*, vol. 14, no. 1, Feb. 2017, Art. no. 016003.

[112] R. T. Schirrmeister, J. T. Springenberg, L. D. J. Fiederer, M. Glasstetter, K. Eggensperger, M. Tangermann, F. Hutter, W. Burgard, and T. Ball, "Deep learning with convolutional neural networks for EEG decoding and visualization," *Hum. Brain Mapping*, vol. 38, no. 11, pp. 5391–5420, Nov. 2017.

[113] S. Sakhavi, C. Guan, and S. Yan, "Learning temporal information for brain-computer interface using convolutional neural networks," *IEEE Trans. Neural Netw. Learn. Syst.*, vol. 29, no. 11, pp. 5619–5629, Mar. 2018.

[114] P. Wang, A. Jiang, X. Liu, J. Shang, and L. Zhang, "LSTM-based EEG classification in motor imagery tasks," *IEEE Trans. Neural Syst. Rehabil. Eng.*, vol. 26, no. 11, pp. 2086–2095, Nov. 2018.

[115] T.-J. Luo, C.-L. Zhou, and F. Chao, "Exploring spatial-frequency-sequential relationships for motor imagery classification with recurrent neural network," *BMC Bioinf.*, vol. 19, no. 1, p. 344, Sep. 2018.

[116] V. J. Lawhern, A. J. Solon, N. R. Waytowich, S. M. Gordon, C. P. Hung, and B. J. Lance, "EEGNet: A compact convolutional neural network for EEG-based brain–computer interfaces," *J. Neural Eng.*, vol. 15, no. 5, Oct. 2018, Art. no. 056013.

[117] A. Hassanpour, M. Moradikia, H. Adeli, S. R. Khayami, and P. Shamsinejadbabaki, "A novel end-to-end deep learning scheme for classifying multi-class motor imagery electroencephalography signals," *Expert Syst.*, vol. 36, no. 6, Dec. 2019, Art. no. e12494.

[118] C. J. Ortiz-Echeverri, S. Salazar-Colores, J. Rodríguez-Reséndiz, and R. A. Gómez-Loenzo, "A new approach for motor imagery classification based on sorted blind source separation, continuous wavelet transform, and convolutional neural network," *Sensors*, vol. 19, no. 20, p. 4541, Oct. 2019.

[119] I. Majidov and T. Whangbo, "Efficient classification of motor imagery electroencephalography signals using deep learning methods," *Sensors*, vol. 19, no. 7, p. 1736, Apr. 2019.

[120] S. Chaudhary, S. Taran, V. Bajaj, and A. Sengur, "Convolutional neural network based approach towards motor imagery," *IEEE Sensors J.*, vol. 19, no. 12, pp. 4494–4500, Feb. 2019.

[121] Y. Li, X.-R. Zhang, B. Zhang, M.-Y. Lei, W.-G. Cui, and Y.-Z. Guo, "A channel-projection mixed-scale convolutional neural network for motor imagery EEG decoding," *IEEE Trans. Neural Syst. Rehabil. Eng.*, vol. 27, no. 6, pp. 1170–1180, Jun. 2019.

[122] Z. Tayeb, J. Fedjaev, N. Ghaboosi, C. Richter, L. Everding, X. Qu, Y. Wu, G. Cheng, and J. Conradt, "Validating deep neural networks for online decoding of motor imagery movements from EEG signals," *Sensors*, vol. 19, no. 1, p. 210, Jan. 2019.

[123] X. Zhao, H. Zhang, G. Zhu, F. You, S. Kuang, and L. Sun, "A multi-branch 3D convolutional neural network for EEG-based motor imagery classification," *IEEE Trans. Neural Syst. Rehabil. Eng.*, vol. 27, no. 10, pp. 2164–2177, Oct. 2019.

[124] G. Xu, X. Shen, S. Chen, Y. Zong, C. Zhang, H. Yue, M. Liu, F. Chen, and W. Che, "A deep transfer convolutional neural network framework for EEG signal classification," *IEEE Access*, vol. 7, pp. 112767–112776, 2019.

[125] H. Wu, Y. Niu, F. Li, Y. Li, B. Fu, G. Shi, and M. Dong, "A parallel multiscale filter bank convolutional neural networks for motor imagery EEG classification," *Frontiers Neurosci.*, vol. 13, p. 1275, Nov. 2019.

[126] B. E. Olivas-Padilla and M. I. Chacon-Murguia, "Classification of multiple motor imagery using deep convolutional neural networks and spatial filters," *Appl. Soft Comput.*, vol. 75, pp. 461–472, Feb. 2019.

[127] S. U. Amin, M. Alsulaiman, G. Muhammad, M. A. Mekhtiche, and M. S. Hossain, "Deep learning for EEG motor imagery classification based on multi-layer CNNs feature fusion," *Future Gener. Comput. Syst.*, vol. 101, pp. 542–554, Dec. 2019.

[128] D. Li, J. Wang, J. Xu, and X. Fang, "Densely feature fusion based on convolutional neural networks for motor imagery EEG classification," *IEEE Access*, vol. 7, pp. 132720–132730, 2019.
[129] D. Zhao, F. Tang, B. Si, and X. Feng, "Learning joint space–time–frequency features for EEG decoding on small labeled data," *Neural Netw.*, vol. 114, pp. 67–77, Jun. 2019.
[130] G. Dai, J. Zhou, J. Huang, and N. Wang, "HS-CNN: A CNN with hybrid convolution scale for EEG motor imagery classification," *J. Neural Eng.*, vol. 17, no. 1, Jan. 2020, Art. no. 016025.
[131] P. Kant, S. H. Laskar, J. Hazarika, and R. Mahamune, "CWT based transfer learning for motor imagery classification for brain computer interfaces," *J. Neurosci. Methods*, vol. 345, Nov. 2020, Art. no. 108886.
[132] X. Tang, W. Li, X. Li, W. Ma, and X. Dang, "Motor imagery EEG recognition based on conditional optimization empirical mode decomposition and multi-scale convolutional neural network," *Expert Syst. Appl.*, vol. 149, Jul. 2020, Art. no. 113285.
[133] X. Zhao, D. Liu, L. Ma, Q. Liu, K. Chen, S. Xie, and Q. Ai, "Deep CNN model based on serial–parallel structure optimization for four-class motor imagery EEG classification," *Biomed. Signal Process. Control*, vol. 72, Feb. 2022, Art. no. 103338.
[134] M. T. Sadiq, M. Z. Aziz, A. Almogren, A. Yousaf, S. Siuly, and A. U. Rehman, "Exploiting pretrained CNN models for the development of an EEG-based robust BCI framework," *Comput. Biol. Med.*, vol. 143, Apr. 2022, Art. no. 105242.
[135] B. Sun, Z. Wu, Y. Hu, and T. Li, "Golden subject is everyone: A subject transfer neural network for motor imagery-based brain computer interfaces," *Neural Netw.*, vol. 151, pp. 111–120, Jul. 2022.
[136] S. Abenna, M. Nahid, and A. Bajit, "Motor imagery based brain-computer interface: Improving the EEG classification using delta rhythm and LightGBM algorithm," *Biomed. Signal Process. Control*, vol. 71, Jan. 2022, Art. no. 103102.
[137] Y. Han, B. Wang, J. Luo, L. Li, and X. Li, "A classification method for EEG motor imagery signals based on parallel convolutional neural network," *Biomed. Signal Process. Control*, vol. 71, Jan. 2022, Art. no. 103190.
[138] Z. Khademi, F. Ebrahimi, and H. M. Kordy, "A transfer learning-based CNN and LSTM hybrid deep learning model to classify motor imagery EEG signals," *Comput. Biol. Med.*, vol. 143, Apr. 2022, Art. no. 105288.
[139] K. Wang, F. Tian, M. Xu, S. Zhang, L. Xu, and D. Ming, "Resting-state EEG in alpha rhythm may be indicative of the performance of motor imagery-based brain–computer interface," *Entropy*, vol. 24, no. 11, p. 1556, Oct. 2022.
[140] X. Li, J. Chen, N. Shi, C. Yang, P. Gao, X. Chen, Y. Wang, S. Gao, and X. Gao, "A hybrid steady-state visual evoked response-based brain-computer interface with MEG and EEG," *Expert Syst. Appl.*, vol. 223, Aug. 2023, Art. no. 119736.
[141] D. Wen, X. Lang, H. Zhang, Q. Li, Q. Yin, Y. Chen, and Y. Xu, "Task and non-task brain activation differences for assessment of depression and anxiety by fNIRS," *Frontiers Psychiatry*, vol. 12, Nov. 2021, Art. no. 758092.
[142] W. Burde and B. Blankertz, "Is locus control reinforcement a predictor brain-computer interface performance?" in *3rd Int. Brain-Comput. Interface Workshop Training Course*. Graz, Austria: Verlag der Technischen Universität Graz, 2006, pp. 76–77.
[143] E. M. Hammer, S. Halder, B. Blankertz, C. Sannelli, T. Dickhaus, S. Kleih, K.-R. Müller, and A. Kübler, "Psychological predictors of SMR-BCI performance," *Biol. Psychol.*, vol. 89, no. 1, pp. 80–86, Jan. 2012.
[144] T. F. D. Kanthack, A. Guillot, M. Clémençon, U. Debarnot, and F. D. Rienzo, "Effect of physical fatigue elicited by continuous and intermittent exercise on motor imagery ability," *Res. Quart. Exercise Sport*, vol. 91, no. 3, pp. 525–538, Jul. 2020.
[145] F. Lotte and C. Jeunet, "Defining and quantifying users' mental imagery-based BCI skills: A first step," *J. Neural Eng.*, vol. 15, no. 4, Aug. 2018, Art. no. 046030.
[146] M. Ahn, H. Cho, S. Ahn, and S. C. Jun, "High theta and low alpha powers may be indicative of BCI-illiteracy in motor imagery," *PLoS ONE*, vol. 8, no. 11, Nov. 2013, Art. no. e80886.
[147] M. Lee, J.-G. Yoon, and S.-W. Lee, "Predicting motor imagery performance from resting-state EEG using dynamic causal modeling," *Frontiers Hum. Neurosci.*, vol. 14, p. 321, Aug. 2020.
[148] N. Padfield, J. Zabalza, H. Zhao, V. Masero, and J. Ren, "EEG-based brain-computer interfaces using motor-imagery: Techniques and challenges," *Sensors*, vol. 19, no. 1423, pp. 1–34, 2019.
[149] F. Miralles, E. Vargiu, S. Dauwalder, M. Solà, G. Müller-Putz, S. C. Wriessnegger, A. Pinegger, A. Kübler, S. Halder, I. Käthner, S. Martin, J. Daly, E. Armstrong, C. Guger, C. Hintermüller, and H. Lowish, "Brain computer interface on track to home," *Sci. World J.*, vol. 2015, Oct. 2015, Art. no. 623896.
[150] V. Vimala, K. Ramar, and M. Ettappan, "An intelligent sleep apnea classification system based on EEG signals," *J. Med. Syst.*, vol. 43, no. 2, pp. 1–9, Feb. 2019.
[151] F. M. Garcia-Moreno, M. Bermudez-Edo, J. L. Garrido, and M. J. Rodríguez-Fórtiz, "Reducing response time in motor imagery using a headband and deep learning," *Sensors*, vol. 20, no. 23, p. 6730, Nov. 2020.
[152] W. Xiong and Q. Wei, "Reducing calibration time in motor imagery-based BCIs by data alignment and empirical mode decomposition," *PLoS ONE*, vol. 17, no. 2, Feb. 2022, Art. no. e0263641.
[153] S. Selim, M. Tantawi, H. Shedeed, and A. Badr, "Reducing execution time for real-time motor imagery based BCI systems," in *Proc. Int. Conf. Adv. Intell. Syst. Inform.* Cham, Switzerland: Springer, 2017, pp. 555–565.
[154] M. Rashid, B. S. Bari, M. J. Hasan, M. A. M. Razman, R. M. Musa, A. F. Ab Nasir, and A. P. P. A. Majeed, "The classification of motor imagery response: An accuracy enhancement through the ensemble of random subspace k-NN," *PeerJ Comput. Sci.*, vol. 7, p. e374, Mar. 2021.
[155] D. J. McFarland and J. R. Wolpaw, "Brain-computer interfaces for communication and control," *Commun. ACM*, vol. 54, no. 5, pp. 60–66, 2011.
[156] M. Abo-Zahhad, S. M. Ahmed, and S. N. Abbas, "State-of-the-art methods and future perspectives for personal recognition based on electroencephalogram signals," *IET Biometrics*, vol. 4, no. 3, pp. 179–190, Sep. 2015.
[157] S. M. Alarcão and M. J. Fonseca, "Emotions recognition using EEG signals: A survey," *IEEE Trans. Affect. Comput.*, vol. 10, no. 3, pp. 374–393, Jul. 2019.
[158] R. K. Mehta and R. Parasuraman, "Neuroergonomics: A review of applications to physical and cognitive work," *Frontiers Hum. Neurosci.*, vol. 7, p. 889, Dec. 2013.
[159] A. Vaswani, "Attention is all you need," in *Proc. Adv. Neural Inf. Process. Syst.*, vol. 30, 2017, pp. 1–15.